## SOLAR CELLS

Solar cells are devices which convert solar energy directly into electrical energy. These devices are usually made of semiconducting materials, such as silicon or gallium arsenide. Silicon, a group IV element in the periodic table, exhibits properties that lie between a metal (conductor) and an insulator (nonconductor), and therefore falls in the semiconductor category. Semiconductor properties are essential in obtaining solar cell characteristics. Properties of semiconductor materials can be modified by introducing controlled amounts of other materials—commonly referred to as impurities. In silicon, the addi-

tion of group V elements (phosphorus, arsenic, etc.) provides *n*-type impurities, or donors, creating *n*-type silicon (having negative charge carriers, electrons); while the addition of group III elements (boron, aluminium, etc.) provides *p*-type impurities, or acceptors, creating *p*-type silicon (having positive charge carriers, holes). When *n*- and *p*-type silicon are brought together, the resulting interface is called a *p*–*n* junction, and the whole structure is generally called a diode. The junction is the heart of the solar cell and is instrumental in converting sun's energy, in the form of photons, into electrical energy.

The semiconductor material absorbs a large portion of the incoming solar photons, and the device converts their energy to electrical current. A corresponding photovoltage is formed in the device terminals. The absorption process takes place between the valence and conduction bands of the semiconductor. Incoming solar photons excite electrons from the valence band to the conduction band and leave a similar amount of empty states (holes) in the valence band. The minority electrons thus generated in the *p*-type side of the junction diode, as well as the minority holes generated in the *n*-type material, diffuse, on average, a distance that is called the minority carrier diffusion length. If the minority carriers diffuse to the *p*–*n* junction, they are separated by the built-in electric field in the *p*–*n* junction of the device. This phenomenon is called the photovoltaic (PV) effect. The light-generated current is then collected by the front and back metal contacts. The front metal contact is usually patterned in the form of a grid, instead of just a continuous metal layer, to let the incoming light penetrate inside the solar cell. An antireflection coating is also usually deposited on top of the device to prevent losses due to reflection of the light. Figure 1 shows the basic solar cell device structure. In Figure 1, the device has a *p*-on-*n* polarity, which means that the emitter layer is a *p*-type material, and the base layer an *n*-type material.

The photovoltaic effect was first observed by Becquerel in 1839. However, it was not until 1954, 115 years after the discovery of PV effect, that the first practical solar cell device (based on silicon) was developed at Bell Telephone Laboratories (see Refs. 1–3 for the history of the PV effect and solar cells). To fabricate a very simple solar cell, a high concentration of *p* and *n* impurities are diffused into *n* and *p* silicon base substrate, respectively, at high temperatures (900° to 1000°C) to form the junction. Then, front and back metal contacts are deposited. Solar cells can be of any shape; however, circular, square, and rectangular are most common. A typical silicon solar cell produces a voltage of more than 0.5 V and current proportional to solar cell area and intensity of the sunlight. The solar light intensity on the cell surface is sometimes increased by using a lens or a reflector, which together with the cell forms a concentrator system. Various improvements in cell material, design, and processing result in an increase in current-voltage values leading to enhanced energy conversion efficiency.

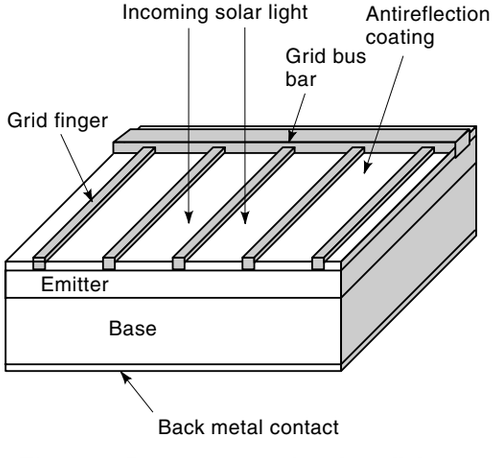


**Figure 1.** Basic structure of a solar cell device.

Solar cells connected in series and/or parallel combinations, referred to as a solar array, are designed to provide specific power requirements. The power produced by solar cells/arrays can be used for various applications, ranging from microwatts to megawatts: that is, from operating a wristwatch to large electric power stations. The photovoltaic or solar cell technology offers several advantages—no need for dependence on depleting fossil fuel, low maintenance, long life, nonpolluting (except possibly during manufacturing), and modularity, as solar cells/arrays can be added anytime to increase power. The drawbacks are low sunlight intensity (1 kW/m$^2$ on Earth's surface, at most), availability during daytime only, and high cost per unit power in comparison with other energy production methods. However, solar cell prices are decreasing at the same time as their manufacturing capacities are increasing.

## SOLAR RADIATION

Solar radiation consists of a wide spectrum of photons. The largest portion of solar energy is located in the visible part of the solar spectrum, between 300 nm and 700 nm. The photon spectrum follows roughly the spectrum of a black-body emitter at a temperature of about 5800 K. The solar spectrum differs from the black-body spectrum, however, due to solar physics and also due to light absorption and scattering in the Earth's atmosphere. The ultraviolet part of solar radiation is largely absorbed by the ozone layer in the upper atmosphere, and other gases in the atmosphere absorb at other wavelengths.

The solar constant is defined as the power input of solar radiation per unit area at the average Earth's distance from the sun, about 150 million kilometers. The value for the solar constant is 1367 W/m$^2$ (this value varies somewhat depending on the standard used). On the Earth's surface, the power input decreases to below 1000 W/m$^2$. Air mass (AM) number is defined roughly as the amount of atmospheric air masses between the sun and the solar cell. Therefore, in space, the solar spectrum contributing to the solar constant is marked as air-mass zero spectrum (AM0). On the Earth's surface, when the sun is at the zenith, the condition is AM1. A standard test condition is marked as AM1.5, or AM1.5D (D implies direct illumination), and this corresponds to a situation where the sun is 45° from the zenith. One may add the letter "G" to this abbreviation to refer to the global spectrum, in which also the scattered light from the sky is added to the AM1.5D spectrum. The total energy input of the AM1.5G standard spectrum is 962 W/m$^2$, although the standard measurement condi-

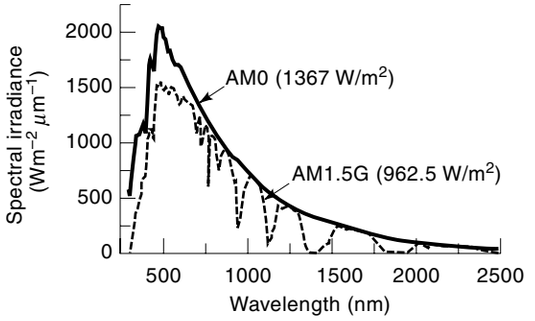


**Figure 2.** Spectral irradiance of the solar light at Earth's distance in space (AM0) and on Earth's surface (AM1.5G). The total power of each spectrum is indicated in parentheses.

tion is 1000 W/m$^2$. Figure 2 shows the most common standard spectra, AM0 and AM1.5G, as a function of photon wavelength. More detailed overview of the solar radiation can be found in Ref. 4.

To utilize the available solar energy efficiently, the semiconductor material for the solar cell has to be chosen in such a way that the energy difference between the semiconductor valence and conduction bands, referred to as the band-gap energy of the semiconductor, lies within the photon energy band. The band-gap is the most important parameter of the solar cell material. If the band-gap is too wide, most of the solar photons are transmitted through the material and do not get absorbed. On the other hand, if the band-gap is too narrow, most of the photons are absorbed, but a large part of the photon energy is lost as heat. Therefore, the optimum band-gap energy of the semiconductor material is just below the maximum intensity regime, 1 eV to 1.5 eV depending on the air mass of the solar spectrum.

With typical single junction solar cells, a large amount of the incoming solar energy is wasted due to light transmission and heat generation, even with an optimal band-gap of the material. Theoretically, a conversion efficiency of about 30% cannot be exceeded with single junction cells. Due to decreased light transmission and heat generation, improved utilization of the solar energy is expected if more than one solar cell material is used in the device.

## BASIC OPERATION OF A SOLAR CELL

The basic parts of a solar cell are the base and emitter layers. They are doped $n$- and $p$-type in such a way that a $p$–$n$ junction is formed between these layers. The thicker one of these two layers is called the base layer, and the thinner layer, usually on the top part of the device, is called the emitter layer. As an example, we may have an $n$-type base layer and a $p$-type emitter layer. This kind of solar cell is said to have a $p$-on-$n$ polarity. The purpose of the $p$–$n$ junction is to separate the light-generated minority carriers from their counterparts (majority carriers) before they unwantedly recombine with each other. A built-in electric field is automatically formed in the junction; therefore, in the $p$-on-$n$ device, the minority holes generated in the base layer are swept by the electric field to the $p$-type emitter, where they are majority carriers. Similarly, the minority electrons generated in the emitter layer are swept over the $p$–$n$ junction to the $n$-type base layer. The minority carriers are swept over the junction only if their diffusion lengths are long enough. Figure 3 shows the minority carrier generation process and movement in the $p$-on-$n$ type solar cell energy band diagram. In a well-designed solar cell, most of the generated minority carriers are thus collected by the junction before they recombine with the majority carriers. This current, which is formed by the minority carriers swept over the $p$–$n$ junction, is called *photocurrent,* and its direction is that of the reverse of the diode forward current flow. Because the operation of the solar cell is based on the minority carriers, their dynamics is of crucial importance for the device. For minority-carrier devices in general, the diffusion lengths of the minority carriers mostly define the performance of the device.

When the solar cell is connected to an external closed circuit having a load resistor, the photocurrent produces a voltage across the load. The polarity of the load voltage causes the $p$–$n$ junction to be biased in the forward direction. As in the case of any $p$–$n$ junction diode, majority carrier diffusion current ("dark" current) is then formed, and it opposes the light-induced minority carrier current in the solar cell. The increase of the diffusion current is a consequence of the self-biasing induced lowering of the built-in barrier at the junction. Due to the diffusion of the majority holes from the $p$-side and majority electrons from the $n$-side (see Fig. 3) the net current output of the solar cell decreases. Although the output voltage increases at the same time, at some point the output power begins to decrease. With a certain value of the load resistor, the output power of the solar cell has the maximum value. The conversion efficiency of the solar cell is defined at this point as the ratio of the maximum electrical output power of the solar cell and of the input light power. Typically, the conversion efficiency may vary from 5% to 30%, depending on the semiconductor material and its crystal quality.

## FUNDAMENTAL SOLAR CELL PARAMETERS

### Quantum Efficiency

The quantum efficiency (QE) of a solar cell describes how many electron–hole pairs are collected by the device with one

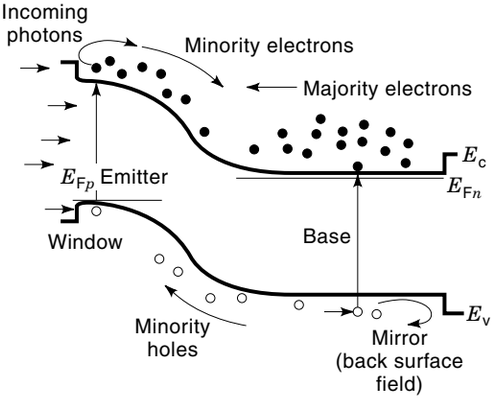


**Figure 3.** Energy band diagram of a solar cell device. Incoming photons generate excess minority carriers (electrons and holes), which are collected by the electric field in the $p$-$n$ junction. The window and mirror layers prevent minority carrier recombination at front and back surfaces of the device: $E_c$ = conduction band minimum, $E_v$ = valence band maximum, $E_{Fp}$ and $E_{Fn}$ are quasi-Fermilevels in the $p$-type emitter and $n$-type base layers, respectively.

single photon, having a definite wavelength $\lambda$. The quantum efficiency is usually shown as a function of photon wavelength. The electron-hole pairs generated at each wavelength sum up to the photocurrent of the device; therefore, the quantum efficiency shows also the solar cell's capability of producing electrical current. Basically, ideal photovoltaic conversion yields one electron-hole pair for each photon, and therefore the maximum value for the quantum efficiency at any wavelength is equal to one. The quantum efficiency may describe either external or internal photovoltaic conversion. The external quantum efficiency ($\eta_e$) is defined on the basis of taking into account all photons entering the cell surface, and it is therefore decreased due to reflection from the surface and from the front metal grid. In the internal quantum efficiency ($\eta_i$), only those photons which penetrate inside the solar cell are taken into account. The external quantum efficiency therefore describes the general behavior of the solar cell device, and the internal QE describes more the solar cell semiconductor material quality. If one considers the active area of the solar cell not covered by the front metal grid, the only difference between the external and internal quantum efficiencies is due to reflection ($R$) from the active area front surface, or $\eta_e(\lambda) = [1 - R(\lambda)]\eta_i(\lambda)$.

At very short wavelengths, light reflection from the cell surface becomes dominant. This is one reason why the external quantum efficiency decreases rapidly below about 400 nm. At long wavelengths, which correspond to photons having energies less than the band-gap of the semiconductor material, the quantum efficiency drops to zero because no electron-hole pairs can be generated by these photons due to their transmission. Between these wavelengths, the internal QE can be nearly one. The QE is decreased, however, if minority carrier recombination takes place in the bulk material, at the interfaces, or at the surfaces of the device.

Because the penetration length of the photons strongly depends on the photon wavelength, and because photocarriers generated deep in the device usually have to travel farther before being collected by the built-in field, by evaluating the quantum efficiency curve one can reach conclusions on the material and interface quality as a function of depth of the device. Therefore, quantum efficiency characterization is a powerful tool for analyzing solar cells. For example, one can compare the quantum efficiencies of silicon cells having good and bad crystal qualities and see that the diffusion length of the minority carriers decreases due to crystal defects. The degradation can be seen in the long wavelength regime (Fig. 4), because the photocarriers generated deep in the cell must travel to the junction and often they recombine at the crystal defects first. In GaAs solar cells, the deteriorating effect of front surface recombination at short wavelengths can be seen by comparing quantum efficiencies of cells with and without a window layer (Fig. 5).

## FUNDAMENTAL SOLAR CELL PARAMETERS

Operation of the solar cell is based on the generation of photocurrent under light bias conditions. To calculate the photocurrent density of a solar cell, one needs information about the quantum efficiency of the cell as well as the air mass conditions (solar spectrum).

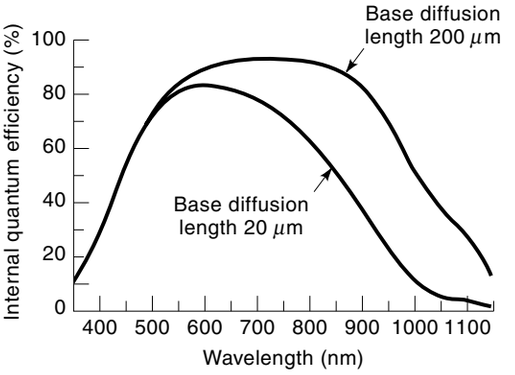


**Figure 4.** Internal quantum efficiencies of Si solar cells with different minority carrier diffusion lengths in the base. The photogenerated minority carrier collection of the device is enhanced if the diffusion length in the base is increased.

By multiplying the quantum efficiency with the intensity of the solar radiation at each wavelength and integrating the results over the whole solar spectrum, one obtains the photogenerated carrier current density, or the photocurrent density

$$J_L = q \int_0^\infty F(\lambda)\eta_e(\lambda)\, d\lambda \tag{1}$$

where $q$ is the elementary charge, and $F(\lambda)$ is the incoming photon flux. If a solar cell consists of an ideal $p$–$n$ junction, the output current characteristics of the device is a sum of the constant photocurrent and the opposing exponentially varying forward diffusion current. In the case of an ideal $p$–$n$ junction, the solar cell voltage–current ($IV$) characteristics can be drawn by shifting the dark $IV$ curve along the current axis by the amount of photocurrent (Fig. 6). The photocurrent is opposed by the forward diffusion current over the $p$–$n$ junction, and by the recombination current in the space charge region of the diode. For simplicity, the ideal diode diffusion current is considered first. In a real solar cell device the recombination currents in the depletion region, interfaces, and surfaces play important roles as well, and are treated

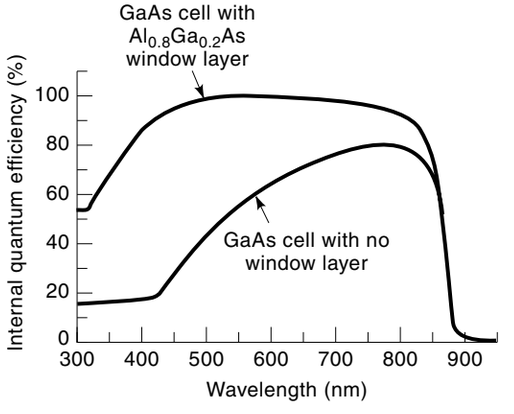


**Figure 5.** Effect of surface passivation in the internal quantum efficiency of GaAs solar cells. The high surface recombination velocity of GaAs deteriorates the QE in the short wavelength range if AlGaAs window layer is not used.

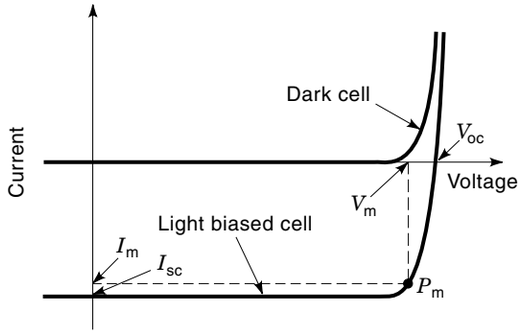


**Figure 6.** Voltage-current characteristics of a solar cell in dark and under light illumination conditions: $P_m$ is the maximum output power of the cell, with a voltage $V_m$ and current $I_m$; $V_{oc}$ and $I_{sc}$ are the open circuit voltage and short circuit current, respectively.

later. More detailed discussions on the solar cell theory can be found, for example, in Refs. 5–7. The total current density from the solar cell device, in the case of no recombination currents, is

$$J = J_0[\exp(qV/kT) - 1] - J_{ph} \tag{2}$$

where $V$ is the bias voltage of the junction, $k$ is the Boltzmann constant, $T$ is the absolute temperature, and

$$J_0 = kTn_i^2\left[\frac{\mu_e}{L_eN_A} + \frac{\mu_h}{L_hN_D}\right] \tag{3}$$

is the reverse saturation current of the diode. In Equation (3), $\mu_e$ and $\mu_h$ are the electron and hole mobilities, $N_A$ and $N_D$ are the acceptor and donor densities in the $p$–$n$ junction, $L_e$ and $L_h$ are the minority electron and hole diffusion lengths, and $n_i$ is the intrinsic carrier concentration of the semiconductor, expressed as

$$n_i = N_CN_V \exp(-E_g/kT) \tag{4}$$

where $N_C$ and $N_V$ are the effective state densities for conduction band and valence band, respectively, and $E_g$ is the semiconductor band-gap energy.

The minority carrier diffusion lengths are related to the minority carrier lifetimes $\tau_e$ and $\tau_h$ through the formulae $L_e^2 = D_e\tau_e$ for electrons, and $L_h^2 = D_h\tau_h$ for holes. $D_e$ and $D_h$ denote to the electron and hole diffusion coefficients, respectively. The minority carrier diffusion length (and corresponding lifetime) is the most important parameter describing solar cell material quality for photovoltaic application.

The equivalent circuit of the solar cell is shown in Fig. 7. The current generator in the circuit represents the light-generated photocurrent, and the diode in the circuit represents the unilluminated dark behavior of the $p$–$n$ junction.

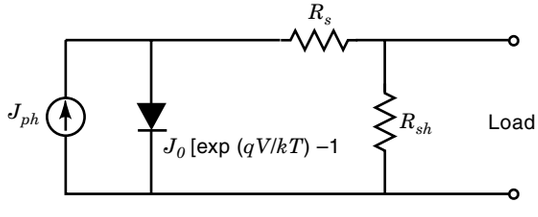


**Figure 7.** Equivalent circuit of a solar cell.

The open-circuit voltage $V_{oc}$ of the solar cell is defined as the voltage where the diffusion current and photocurrent exactly cancel each other: that is, the output current is zero. Therefore, one obtains by solving $V_{oc}$ from Eq. (2),

$$V_{oc} = \frac{kT}{q}\ln\left(\frac{J_{ph}}{J_0} + 1\right) \tag{5}$$

The amount of the forward diffusion current in the junction is controlled by the magnitude of the resistive load that is connected to the solar cell (see equivalent circuit in Fig. 7). The net output current decreases with increasing load resistances due to increased voltage across the load, which increases the diffusion current exponentially. Because the power output of the solar cell is the output current multiplied by the output voltage, there is a maximum output power, $P_m$, which is equal to the product of the maximum power-point current $I_m$ and the maximum power-point voltage $V_m$ (Fig. 6).

The maximum possible current with a given light bias is obtained when the solar cell is short-circuited (load resistance is zero). This current is called the short-circuit current $I_{sc}$ of the solar cell, and it is always larger than $I_m$. Similarly, the maximum possible output voltage is obtained when the external circuit is open-circuited (load resistance is infinite). The open-circuit voltage is always larger than the maximum power-point voltage $V_m$.

Typically, one tries to maximize the fill factor (FF), which describes the squareness of the *IV* characteristics between zero voltage and $V_{oc}$.

The fill factor of the solar cell is defined as

$$FF = \frac{V_mJ_m}{V_{oc}J_L} \tag{6}$$

where $J_m = I_m/A$ is the output current density of the cell at the maximum power point ($A$ is the device area). The fill factor, in the ideal case, depends only on the magnitude of the dark diffusion current, and therefore on the reverse saturation current. In a real diode, series and shunt resistances, as well as recombination currents and other nonideal effects, also make contributions to the fill factor.

The conversion efficiency $\eta$ is the most important parameter of a solar cell. It is defined as the ratio of the electrical output power to the input light power $P_i$ of the solar cell, or

$$\eta = \frac{V_mI_m}{P_i} \tag{7}$$

It is important to note that the conversion efficiency of a solar cell depends strongly on the solar spectrum and on the light intensity. In addition, the temperature of the solar cell has an effect on $\eta$ due to the temperature dependence of $J_0$. Increased $J_0$ causes increase in the dark current, leading to reduction in fill factor, open-circuit voltage, and conversion efficiency. Typically, the conversion efficiency of the solar cell increases with decreasing temperature, increasing air mass, and increasing light intensity.

## LOSSES AND CELL OPTIMIZATION

### Recombination

Recombination of the light-generated minority carriers may take place in several regions within the solar cell, causing the photocurrent to decrease. Bulk recombination in the emitter and base layers may be caused by imperfect crystal quality. In amorphous and polycrystalline materials this kind of recombination may be very significant. The crystal defects form deep energy levels in the band-gap. These levels may act as recombination centers, or as "meeting places," for the electrons and holes, and the minority carrier diffusion lengths and lifetimes are decreased due to the increased recombination in these centers. Additional deep energy levels in the band-gap may also be formed by unwanted impurity atoms. If the solar cell is exposed to high-energy particle radiation (usually protons and electrons), damage and deep levels may again occur in the material. This is a usual condition for solar cells used in space conditions (satellites).

Electron–hole recombination that takes place within the depletion region (space charge region) around the $p$–$n$ junction of the cell forms an additional component to the dark current of the diode. This Shockley–Read–Hall (SRH) recombination current can be shown (5) to have the form

$$J_r = \frac{qWn_i}{2\sqrt{\tau_e \tau_h}} \exp\left(\frac{qV}{2kT}\right) = J_{r0} \exp\left(\frac{qV}{2kT}\right) \tag{8}$$

where $W$ is the width of the depletion region of the $p$–$n$ junction.

When Eq. (8) is combined with the ideal diffusion current component, shown in Eq. (2) as the exponential term, the total solar cell equation becomes

$$J = J_0 \exp(qV/kT) + J_{r0} \exp(qV/2kT) - J_{ph} \tag{9}$$

This equation is usually approximated with the formula

$$J = J_s \exp(qV/NkT) - J_{ph} \tag{10}$$

where $N$ is the diode ideality factor, having a value between 1 and 2, and $J_s$ is the reverse saturation current density of the nonideal diode. If the ideality factor is close to 1, the diode is nearly ideal, and the diffusion current dominates the dark behavior. An ideality factor close to 2 indicates strong recombination currents in the depletion region and nonideal material quality.

Surface recombination at the solar cell front surface may have a very important role in destroying the minority carriers that have been generated in the emitter layer. Therefore, surface passivation must be provided for the cell. This can be done by growing a passivating oxide layer (as in the case of silicon solar cells, the passivating native oxide layer grows naturally). In the case of III–V semiconductor solar cells, the surface recombination velocity is normally very high and the native oxide layer does not provide sufficient passivation. Therefore, for III–V solar cells the surface passivation is usually obtained by using a heterojunction barrier for the minority carriers to prevent them entering the surface. This kind of layer is usually referred to as a window layer. As an example, GaAs solar cells usually have an $Al_xGa_{1-x}As$ or a $Ga_{0.51}In_{0.49}P$ wide-gap window layer (5–8). If a heterojunction-based window cannot be applied in a proper way, a graded doping profile in the emitter can be used. Such a profile induces a drift field, which guides the minority carriers towards the $p$–$n$ junction, but it is not so effective as the use of window layers. This method is used in solar cells in which the $p$–$n$ junction is formed by diffusion. A step-graded doping profile has also been used in InP cells (9), for which a proper wide-gap heterojunction window layer material is difficult to find. The effect of strong surface recombination can also be reduced by decreasing the thickness of the emitter layer. At the same time, however, the sheet resistance of the emitter layer increases, causing an increase in series resistance.

As at the front surface, minority carrier recombination may take place at the back surface or at the back interface of the cell. In this case, a barrier for the minority carriers can be formed by using a heterojunction-based mirror layer or just by introducing a heavily doped layer to form a drift electric field, or *back-surface field,* to prevent recombination at the back surface.

In addition to the decrease in the photocurrent, the recombination processes decrease the fill factor of the solar cell as well. For example, deep trap levels in the solar cell material cause a decrease in the fill factor by increasing the SRH-type trap recombination in the depletion region of the $p$–$n$ junction, thereby increasing the reverse saturation current and the diode ideality factor. A similar effect is caused by the shortening of the minority carrier diffusion lengths due to the traps. The interface and surface recombination causes decrease in the fill factor when the cell is light-biased. The effect of the interface recombination on the fill factor cannot be seen directly by summing the photocurrent and the dark current, because the minority carrier distributions are different in dark and light-bias conditions, and therefore different current–voltage characteristics result. The reduced fill factor can only be seen on the actual load $IV$ characteristics of the solar cell.

### Series and Shunt Resistances

The total series resistance of the solar cell consists of the bulk resistances of the semiconductor materials (including the sheet resistance of the emitter layer), interface resistances in the heterojunctions, contact resistances between the semiconductor and the metal layers, and metal-layer resistances (mainly the front grid resistance). Shunt current is caused by leakage currents over the $p$–$n$ junction. Leakage may be caused by defects inside the material, or due to insufficient cell perimeter passivation. In the ideal case, the series resistance should be zero, and the shunt resistance infinite. Series and shunt resistances can be taken into account in the solar cell current equation (although not in explicit form; see Ref. 6):

$$J\left(1 - \frac{R_s}{R_{sh}}\right) - \frac{V}{R_{sh}} = J_s\left[\exp\left(\frac{q(V - JR_sA)}{NkT}\right) - 1\right] - J_{ph} \tag{11}$$

where $R_s$ is the series resistance, and $R_{sh}$ is the shunt resistance. Typically, the shunt resistance is very large, and the

equation is simplified to the form

$$J \approx J_s \left[ \exp\left( \frac{q(V - JR_sA)}{NkT} \right) - 1 \right] - J_{ph} \tag{12}$$

High series resistance and low shunt resistance decrease the fill factor. Low shunt resistance also decreases the voltage of the cell.

There are several regions within the solar cell that contribute to the series resistance. The base layer resistance decreases when the doping level is increased. However, the minority carrier diffusion length in the base layer decreases with increased doping, and a decrease in the photocurrent is therefore expected if too high a doping level is used. The sheet resistance of the emitter layer must be optimized together with the grid, taking into account the decreasing minority carrier diffusion length if the emitter layer doping level is increased. The contact resistances of the cell can be minimized by using proper contact metals having low Schottky barriers. Sometimes a special highly doped cap layer is used between the window layer and the contact metal to decrease the contact resistance, because the contact resistances are usually high if the metal is applied directly to the wide-gap window layer, due to high Schottky barriers. In Fig. 8, current–voltage characteristics for solar cells having ideal and nonideal $p$–$n$ junctions, as well as series and shunt resistances, are shown.

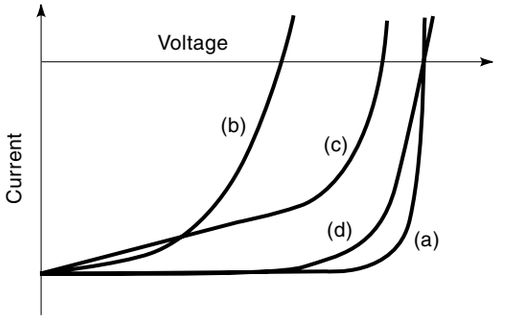


**Figure 8.** Load *IV* characteristics of various solar cells: (a) ideal $p$–$n$ junction, (b) nonideal $p$–$n$-junction, (c) low shunt resistance, (d) high series resistance.

### Grid Obscuration

The electric current generated in the solar cell device is collected by a metal grid, which is patterned on the front surface of the cell (Fig. 1). Usually, the grid consists of narrow fingers that are electrically connected to a metal bar. This grid prevents part of the arriving light from penetrating inside the solar cell. If the grid coverage is made smaller by decreasing the grid and bar widths, the grid resistance increases due to the smaller cross section of the metal patterns. Therefore, the design of the grid pattern is a tradeoff between the resistive losses in the grid and current loss in the cell due to decreased flux of the light penetrating into the device.

The total power losses $P_t$ caused by the grid are

$$P_t = P_o + P_s + P_c + P_f + P_b \tag{13}$$

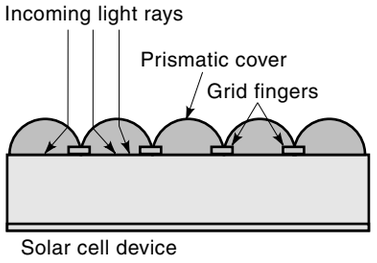


**Figure 9.** The use of a prismatic cover on the solar cell surface minimizes losses which are caused by the grid obscuration.

where $P_o$ is the grid obscuration loss, $P_s$ is the sheet-resistance loss, $P_c$ is the contact-resistance loss, $P_f$ is the finger resistance loss, and $P_b$ is the busbar loss (10). $P_o$ can be minimized by decreasing the finger and busbar areas. The sheet-resistance loss can be minimized either by increasing the emitter layer conductivity (increasing the doping level) or by decreasing the finger separation. Usually the sheet resistance is fixed by the carrier collection properties of the emitter; therefore the only practical method to minimize these losses is the design of the finger separation. The contact resistance is decreased by increasing the grid area. However, this loss is usually negligible except in concentrator applications. Losses caused by the finger resistance and the busbar resistance can be minimized by increasing the cross section of these metal patterns. The maximum height of these patterns is set by the metal deposition method; therefore their width is the only variable in this case. The finger and grid resistance losses can be further decreased if their geometrical forms are designed carefully.

Theoretically, the problem of the grid coverage can be totally avoided if prismatic (Entech) covers are used. The part of the light that would be reflected by the metal grid is refracted into the solar cell by the prismatic cover (Fig. 9). However, in practice, part of the incoming light is additionally absorbed in the prismatic cover, or reflected at the interface of the cell and the cover, and no significant advantage is obtained if the metal grid coverage is small. Addition of the prismatic cover also complicates the manufacturing process and causes extra cost. This kind of cover is therefore advantageous only when the grid coverage is exceptionally large, as may be the case in concentrator solar cells, which produce high photocurrents and in which the grid coverage has to be large to minimize the high resistive losses.

### Reflection

Part of the incoming photons may be reflected from the solar cell surface without entering the semiconductor. Typically, 30% to 40% of the photons are reflected if the semiconductor surface has not been coated. Antireflection (AR) coatings are therefore necessary to avoid this type of loss. The AR coating is usually formed by depositing dielectric materials having refractive indices between 1.3 and 2.6 (see Table 1 for a list of typical AR materials). The coating may consist of one or two, or in some cases even three, layers. By using several layers, the AR properties of the coating can be enhanced, but the manufacture of the solar cell becomes more complex. In the case of single-layer AR coating, the reflection from the solar cell surface may be decreased to less than 20% over the whole

**Table 1. Dielectric Materials Used in Solar Cell AR Coatings**

| Material | Refractive Index | Description |
|---|---|---|
| $MgF_2$ | 1.38 | Used in double-layer coatings with ZnS |
| $SiO_2$ | 1.48 | Plasma-enhanced CVD, used in double-layer coatings with $SiN_x$ |
| $Al_2O_3$ | 1.6 | Used in double-layer coatings with $Ta_2O_5$ |
| $SiN_x$ | 1.9–2.1 | Plasma-enhanced CVD, single-layer AR, double-layer coatings with $SiO_2$ |
| SiO | 2.0 | Single-layer coatings |
| $TiO_2$ | 2.2 | Single-layer and double-layer coatings |
| $Ta_2O_5$ | 2.25 | Used in double-layer coatings with $Al_2O_3$ |
| ZnS | 2.30 | Used in double-layer coatings with $MgF_2$ |

CVD = chemical vapor deposition.

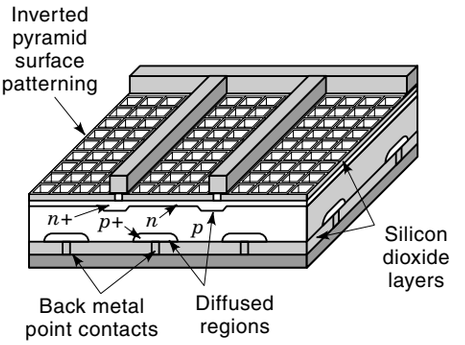


**Figure 11.** Structure of the high-efficiency PERL silicon solar cell: AM1.5G conversion efficiency of 24% has been achieved with this kind of cell (17).

active wavelength range, and in the case of double-layer coating, it may be decreased to less than 5%. As an example, the reflection curve of a silicon solar cell with a one-layer coating is shown in Fig. 10. The same figure shows also the internal and external quantum efficiencies of the solar cell.

In some cell materials, surface texturing can be used to decrease reflection losses by manufacturing *pyramid* structures in the top part of the cell. These pyramids increase the light penetration into the cell, and this kind of AR is less wavelength-dependent. The infrared light rays penetrate inside the cell efficiently, which may decrease the cell conversion efficiency due to cell heating. Surface texturing can be also used to trap light rays in the solar cell in materials that have low absorption coefficient (such as silicon). The textured reflecting layers can be used on both bottom and top sides of the structure. These layers make internal reflection of the light rays possible, and more than 50 reflections for the rays inside the cell can be achieved. The advantages of this kind of structure are that the cell can be made significantly thinner (about ten times) and the effect of bulk recombination in the material becomes less important, which may increase the cell voltage. Surface texturing is a standard process in modern commercial silicon cells. Figure 11 shows an advanced passivated-emitter, rear locally diffused (PERL) silicon cell using inverted pyramidal surface texturing.

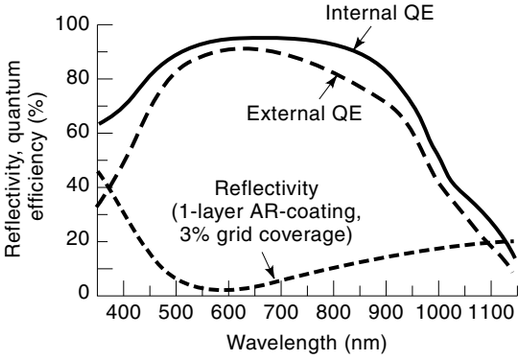


**Figure 10.** Internal and external quantum efficiencies of an Si solar cell. The difference between these two curves is explained by the reflectivity of the light from the surface and from the front grid.

### Design of the Antireflection Coating

The reflection properties of semiconductor materials vary strongly as a function of light wavelength. By using a single-layer AR coating with proper refractive index and thickness, the reflection constant can be dropped to zero at a definite wavelength. For a single-layer AR coating the optimum refractive index can be calculated from the formula

$$n_1 = \sqrt{n_0 n_s} \tag{14}$$

where $n_0$ is the refractive index of the surrounding medium (usually air), and $n_s$ is the refractive index of the substrate. The optimum thickness $d_1$ of the single-layer AR coating can then be calculated as

$$d_1 = \lambda_0 / 4 n_1 \tag{15}$$

where $\lambda_0$ is the wavelength at the maximum response of the solar cell. By increasing the number of layers in the AR coating one can decrease the reflection over a wide range. The reflection coefficient can be calculated from the formula (see also Ref. 11)

$$R = \left(\frac{n_0 - Y}{n_0 + Y}\right)\left(\frac{n_0 - Y}{n_0 + Y}\right)^* \tag{16}$$

where $Y$ is the optical admittance of the layer stack. The optical admittance can be calculated from the equation $Y = C/B$, where the parameters $C$ and $B$ are defined by the formula

$$\begin{pmatrix} B \\ C \end{pmatrix} = \left[\prod_{j=1}^{K} \begin{pmatrix} \cos\delta_j & \frac{i \sin\delta_j}{n_j} \\ i n_j \sin\delta_j & \cos\delta_j \end{pmatrix}\right] \begin{pmatrix} 1 \\ n_s \end{pmatrix} \tag{17}$$

where the refractive indices of the coating layers are denoted by $n_j$, $j = 1,2,3, \ldots, K$; $K$ is the number of the layers in a multilayer coating; and $\delta_j$ is the optical thickness of layer $j$, defined as $\delta_j = (2\pi/\lambda) n_j d_j$, where $d_j$ is the physical thickness of the layer, and $\lambda$ is the photon wavelength. Generally, the optimized AR coating has the layer with the highest refractive index on the bottom and the layer with the lowest refrac-

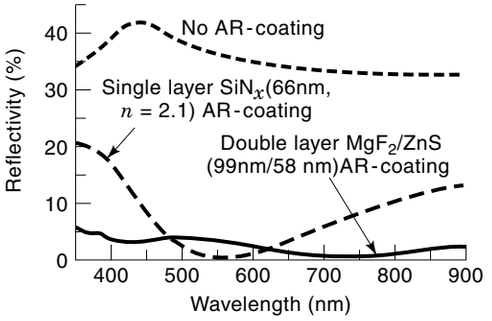


**Figure 12.** Reflectivity of a GaAs solar cell with no AR coating, single-layer AR coating, and double-layer AR coating.

tive index on the top of the AR stack. In Fig. 12, the reflectivity of a GaAs solar cell is shown with various AR coatings.

The main reason for having an AR coating on the solar cell is to increase the photocurrent generated in the device. Therefore, one should optimize the AR coating according to the spectral response properties of the cell. Low reflection is important at wavelengths near the maximum of the solar spectrum and of the internal QE.

To find the maximum possible conversion efficiency for the photovoltaic solar energy conversion is not an easy task, because one has to make assumptions about the development of the material quality of present materials, as well as of the availability of new materials in the future. The material quality depends significantly on the method which is used to produce it; to improve the material quality might implicate that better and more expensive production methods should be used, making the solar cell not commercially competitive, and therefore it would loose our interest. This can be clearly seen from the various approaches of the manufacturing of silicon-based solar cell devices. To assess the possibility for having new materials in the future available for solar cells is also difficult, because new semiconductor materials are invented at a fast pace, but the transfer process from the laboratory to production usually takes several years. However, a realistic and still interesting approach to evaluate maximum photovoltaic conversion efficiencies might be the evaluation of the possibilities to improve the existing materials used by the photovoltaic community. For this purpose, all the parameters which are limiting the present day conversion efficiencies have to be examined.

### Ideal Band-Gap of the Solar Cell Material

When choosing the ideal band-gap for a single-junction solar cell, a trade-off must be made between the photon transmission and the phonon emission processes. The narrower the band-gap is, the more light is absorbed because all radiation which has higher energy than the band-gap is absorbed, considering that the absorbing material is thick enough. However, decreasing the material band-gap leads to larger power losses due to phonon emission processes of the minority carriers. Phonon emission takes place when the generated minority electrons or holes collide with semiconductor lattice atoms. If the photon energy is larger than the band-gap energy of the semiconductor, the additional energy is absorbed and lost to lattice vibrations (i.e., phonons) through these collisions. This process takes place faster than the minority carrier collection over the $p$–$n$ junction. By making an optimal trade-off between the transmission and phonon processes, the ideal band-gap for the maximum possible conversion efficiency of the solar cell material can be calculated. The optimum band-gap for single-junction photovoltaic conversion is about 1.3 eV. In Fig. 13, theoretical maximum conversion efficiencies for single junction photovoltaic conversion are shown as a function of semiconductor band-gap for AM0 and AM1.5G spectra.

Photon transmission and phonon emission are among the most important loss mechanisms in solar cells. Theoretically, both of them can be decreased by using multiband-gap structures such as heterojunction or multijunction solar cells structures. When using various band-gap materials in the solar cell structure, the photons with different energies can be absorbed with smaller phonon emission losses. In this kind of structures one can also use materials with narrow band-gaps to reduce the transmission losses.

### Current Collection Optimization

As seen from Eq. (1), one obtains the photocurrent of a solar cell by multiplying the quantum efficiency and the solar spectral intensity and integrating the product over all relevant wavelengths. Therefore, to maximize the photocurrent, one should maximize the wavelength range covered by the quantum efficiency. There are several factors which influence the magnitude of the quantum efficiency.

Basically, the maximum current from a solar cell one obtains by minimizing the band-gap; therefore, the wavelength covered by the quantum efficiency would be extended to longer wavelengths. However, one has to take into account the subsequent decrease of the voltage and to find the optimum trade-off. With the optimized band-gap material, one can increase the photocurrent by increasing the thickness of the absorbing layer (typically, base layer). If the material has indirect band-gap, like silicon, the thickness of the absorbing layer should be of the order of 200 to 500 $\mu$m. In the case of direct-gap semiconductors, like GaAs and InP, most of the light is absorbed with a thickness of only 2 to 5 $\mu$m.

Other factors contributing to the quantum efficiency, and therefore to the photocurrent, are the minority carrier diffusion lengths and corresponding lifetimes. If the diffusion lengths are short (for example, in the base layer, less than the layer thickness), a large fraction of the minority carriers

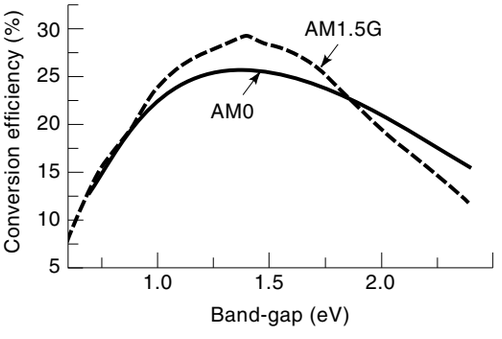


**Figure 13.** Theoretical conversion efficiencies of solar cells as a function of the band-gap energy of the semiconductor material. Higher conversion efficiency can be achieved in AM1.5G conditions than AM0 conditions due to smaller phonon absorption losses with the AM1.5G spectrum. Data obtained from Ref. 7.

are lost through recombination in the bulk before they are collected by the junction. The diffusion length is strongly dependent on the defect density in the material. Imperfect crystal quality, as well as unwanted deep level impurities, causes SRH-type bulk recombination through the induced trap levels. At low illumination (1-sun intensity), the SRH-lifetime for minority electrons has the form (12)

$$\tau_n = \frac{1}{c_n N_t} \tag{18}$$

where $c_n = \sigma_n \langle v_t \rangle$ is the electron capture coefficient ($\sigma_n$ is the minority electron capture cross section, and $v_t$ is the electron thermal velocity), and $N_t$ is the trap level density. A corresponding expression exists for minority holes. Radiative recombination of photocarriers is increased if the doping level is increased in direct-gap materials. The expression for the radiative lifetime with low light illumination level is (12)

$$\tau_r = \frac{1}{B(n+p)} \tag{19}$$

where $B$ is the material-dependent rate of radiative capture probability, $n$ is the electron concentration, and $p$ is the hole concentration of the material.

At very high doping densities (generally well above $10^{18}$ $cm^{-3}$), Auger recombination may cause additional decrease for the lifetime and for the diffusion length, especially in the emitter layer, which is usually highly doped. The minority electron and hole lifetimes ($\tau_e$ and $\tau_h$) can then be calculated as an inverse sum of all these recombination lifetimes $\tau_i$, or (for electrons)

$$\tau_e^{-1} = \sum \tau_i^{-1} \tag{20}$$

The corresponding minority carrier diffusion length can then be calculated. In addition to the effect of low bulk material lifetimes, the photocurrent is also decreased if the surface and interface recombination velocities are high. The effect of the surface and interface recombination can be approximated by the formula (for electrons)

$$\frac{1}{\tau_{eff}} = \frac{1}{\tau_e} + \frac{S_f + S_b}{D_e} \tag{21}$$

where the effects of the front and back interface (or surface) recombination velocities $S_f$ and $S_b$ have been taken into account as contributions to the effective minority carrier lifetime $\tau_{eff}$.

In the case of direct-gap semiconductors, the effect of radiative recombination is decreased by the effect known as *photon recycling*. This means a situation where a photon, created by radiative electron–hole recombination, is absorbed in the solar cell and contributes to the minority carrier generation. Basically, photon recycling can be taken into account in the design of the solar cell structure by increasing the internal reflection of the photons trying to escape from the cell's active layers. This can be made by using Bragg reflector structures, for example, at the back interface of the solar cell base layer. The Bragg reflectors are tuned to be most effective for photons with the band-gap energy. The manufacturing of Bragg reflectors is, however, difficult.

### Voltage Optimization

Basically, optimizing the maximum power-point voltage $V_m$ implicates the maximum possible values for the open-circuit voltage $V_{oc}$, and for the fill-factor. As seen in Eq. (5), the open-circuit voltage is strongly dependent on the reverse saturation current density $J_0$ of the $p$–$n$ junction. The reverse saturation current depends strongly on the intrinsic carrier density (Eq. 4), which is an exponential function of the band-gap of the semiconductor. The wider the band-gap is, the higher is the voltage. However, increasing the width of the band-gap causes decrease in the photocurrent due to increased transmission losses.

In addition, the reverse saturation current depends on three bulk factors of the semiconductor, the doping levels, diffusion lengths, and mobilities in the base and emitter layers, as seen from the formula of the reverse saturation current (Eq. 3). To maximize the voltage output of the solar cell, one should decrease the reverse saturation current as much as possible. The reverse saturation current decreases by increasing the doping levels and the diffusion lengths, and by decreasing the mobilities in the base and emitter layers. Usually, increasing the doping level causes decrease in the semiconductor material mobilities, but at the same time the diffusion lengths decrease as well, which decreases the photocurrent. Therefore, one has to find an optimized trade-off between the maximum possible doping levels and diffusion lengths. In a balanced situation, the order of magnitude of the emitter layer doping level is about $10^{18}$ $cm^{-3}$, and the base layer doping level is about $10^{17}$ $cm^{-3}$.

### Multiband-Gap Structures

The maximum theoretical conversion efficiency for a single-junction solar cell made of one material is about 30%. Significantly higher efficiencies of the solar cells are expected if the photon transmission and phonon emission processes are decreased by distributing the current generation to more than one material. Basically, there exist two ways to combine the different materials, heterojunction and multijunction solar cell structures.

**Heterojunction Solar Cells.** In the heterojunction solar cells, the $p$-$n$ junction is formed between two different materials (6). The lower material layer (base) is made of narrow-gap semiconductor, and the upper layer (called emitter or window) is made of wide-gap semiconductor. In this structure, the high-energy photons are absorbed in the upper layer and the low-energy photons in the lower layer. With this structure, the phonon emission losses are, in theory, decreased by having the absorbing layer band-gap energies better matched with the incoming photon energies. In addition, the transmission losses are smaller because the lower layer band-gap energy may be smaller than in typical homojunction structures. The energy-band diagram of a thin-film heterojunction solar cell is shown in Fig. 14.

The heterojunction interface quality is never perfect, however. Therefore, recombination current is larger than in typical homojunctions and the efficiencies of this kind of cell have remained lower than in the best homojunction cells. A typical example of a heterojunction solar cell is indium-tin-oxide (ITO) and indium phosphide based structure. In this cell, ITO layer may, in addition of being the window layer, act as a

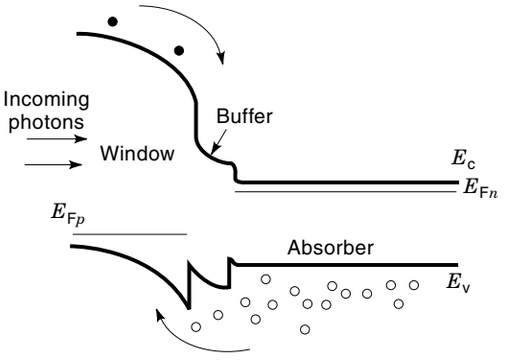


**Figure 14.** Energy band diagram of a heterojunction thin-film solar cell structure. The buffer layer is used to decrease the amount of hazardous misfit dislocations at the heterojunction: $E_c$ and $E_v$ are the conduction and valence band edges, respectively; and $E_{Fp}$ and $E_{Fn}$ are the quasi-Fermilevels in the window and absorber layers, respectively.

replacement of the contact grid due to its high conductance properties.

**Multijunction Solar Cells.** The highest reported solar cell conversion efficiencies have been obtained with multijunction structures (also called cascade solar cells; multijunction cells which have two junctions are called tandem solar cells). These cells may be divided into two major classes, in monolithic multijunction cells and mechanically stacked multijunction cells. As in the case of heterojunction solar cells, the wide-gap material is located on the top part of the device, but in this case it forms a complete junction structure and is named the top cell of the multijunction device. The lowest cell in the stack has the narrowest band-gap. As an example, the absorbable power of the single-junction GaAs cell is compared to the absorbable power of the triple-junction GaInP/GaAs/Ge structure in Fig. 15. A monolithic multijunction cell is typically deposited or epitaxially grown on a single substrate. The structure consists of two or more homojunction solar cell structures (subcells) connected in series (Fig. 16). The additional $p$–$n$ junction forming the connection between the subcells must be a tunnel junction to achieve a small voltage drop and minimize losses. The tunneling current flows directly between the conduction and valence bands of the semiconductor, thus avoiding the voltage drop caused by the junction barrier. However, if the tunneling layer material band-gap is narrower than or as wide as the lower subcell band-gap, additional light absorption and photocurrent losses occur in the tunnel diode. Typically, the cell has only two output connections (terminals) in a similar manner as single junction cells. Due to the series connection, the subcells must be designed in such a way that they are current matched (all cells generate the same amount of current), because the output current of the cell is limited by the less photocurrent-producing cell. In mechanically stacked cells there are typically four terminals, so that current matching condition is not needed in the cell level. However, to get maximum power output in these structures, current or voltage matching is needed in the module or panel level. By increasing the number of junctions (and materials having different band-gaps), one may theoretically improve the reachable efficiency of multijunction cells from about 50% with two junctions to about 72% with 36 junctions (at AM1.5G conditions) (6).

The growth process of the monolithic multijunction cells is significantly more difficult than the single-junction process. Due to the need for current matching, one has to have good control of the growth rates of the subcells, because the light is distributed to the various subcells by adjusting the layer thicknesses. In some cases, the current matching is controlled by varying the material band-gap energies. Only small variation in the subcell quantum efficiencies from growth to growth is allowed, also due to the need for current matching. To make good quality tunnel diodes one has to achieve high doping levels and low diffusion for the tunnel layer dopants. In mechanically stacked structures problems may develop from the construction of the mechanical stack as well as the combination of the cells in the module or panel level. All these factors related to multijunction structures may cause decreased yields in the solar cell or panel manufacturing processes, in comparison with corresponding single-junction processes.

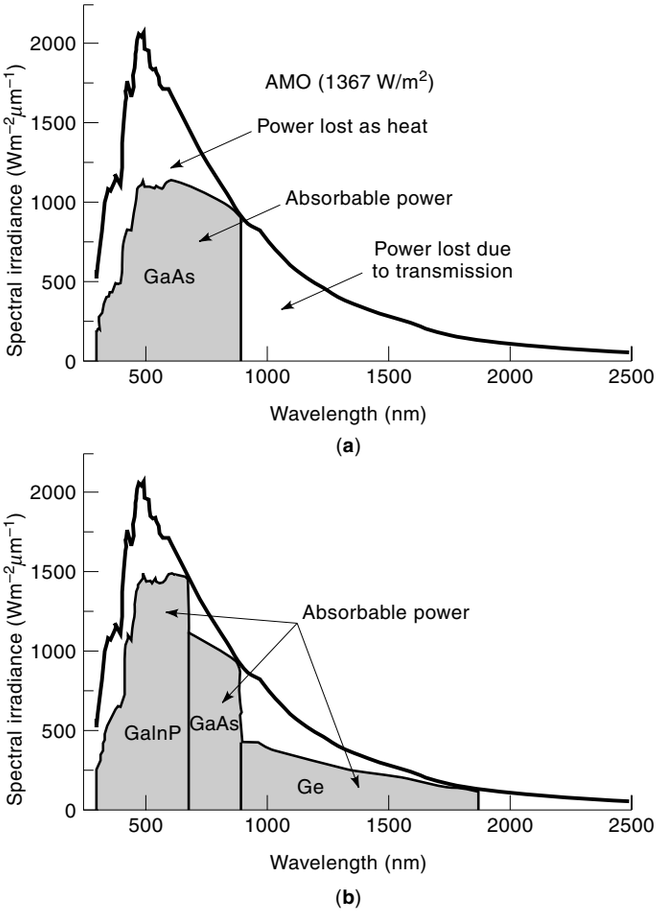


**Figure 15.** Comparison of the absorbable power in a single junction GaAs solar cell (a) and three-junction GaInP/GaAs/Ge cascade solar cell (b). The area below the AM0 curve describes the whole spectral energy of the solar radiation, and the shadowed areas mark the theoretical absorbable part of the solar radiation with the semiconductor materials. The phonon absorption and transmission losses can be decreased with multijunction structures.

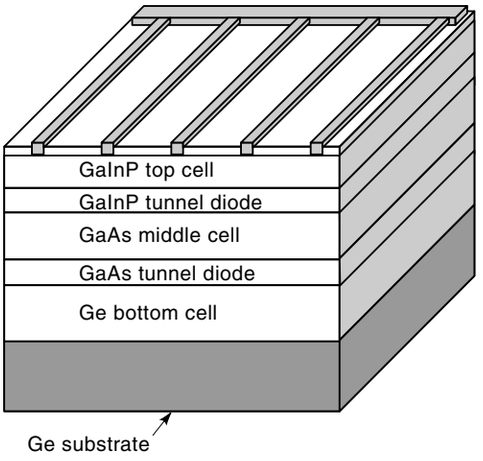


**Figure 16.** Basic structure of a triple-junction GaInP/GaAs/Ge solar cell. The top, middle, and bottom cells are connected electrically by tunnel junctions. This cell has only two terminals as a normal single-junction solar cell.

Typically multijunction cell structures are based on compound semiconductors, although a triple-junction cell based on amorphous silicon and related materials has been demonstrated (13). The best mechanically stacked multijunction cell is based on the GaAs/GaSb structure (14) (Fig. 17). The first monolithic multijunction cell which has achieved over 30% efficiency under unconcentrated AM1.5G conditions is based on the GaInP/GaAs structure (15,16). This structure also has interest in concentrator applications.

## SOLAR CELL MATERIALS AND STRUCTURES

Historically, there have been two main applications where solar cells have been used. The first practical solar cells were developed mainly for space applications in the 1950s. Powering satellites was the most important use until the energy crisis in the early 1970s. Since then, terrestrial applications have gained increased research and commercial interest, and nowadays the production volume of terrestrial cells is much larger than that of space cells.

Solar cells can also be categorized in different groups according to the material they are made of. There are several points that contribute to the choice of the solar cell material. The conversion efficiency, manufacturing cost, and long-term stability are the most important criteria in terrestrial applications, but for space solar cells such material properties as good radiation resistance and light weight are required in addition. At the panel level one may summarize these requirements as the need for minimizing the cost-to-power ratio for terrestrial panels and maximizing the power-to-mass ratio for space panels. There does not exist a material that is superior according to all these criteria. Therefore, one has to make trade-offs and to take into account the needs of the specific application where the solar cells are used. Typically, the solar cell materials are categorized into three main groups, silicon (single crystal and multicrystalline), thin film materials (amorphous and polycrystalline), and crystalline compound semiconductors (mainly for space applications).

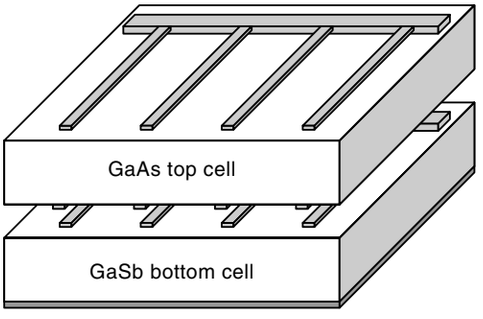


**Figure 17.** Mechanically stacked double-junction GaAs/GaSb solar cell. This kind of multijunction cell has four terminals, two for both top and bottom cells.

### Silicon-based Solar Cells

Silicon is one of the most abundant elements on the earth, found in oxide form as sand. This makes it a very cheap semiconductor material for solar cells, although the need for high purity enormously increases its cost. It is extensively used in the semiconductor industry because it is the best-studied material, its process technology is mature, and it is nontoxic and therefore environmentally safe.

According to crystal quality, silicon can be divided into four main classes: crystalline silicon, multicrystalline silicon (grain size 1 mm to 100 mm), polycrystalline silicon (grain size 1 $\mu$m to 1 mm), and amorphous silicon, in the order of decreasing extent of crystalline order (amorphous silicon, used mostly in hydrogenated form, is usually categorized as a thin film material.

Silicon is an indirect band-gap semiconductor. In this type of material the absorption coefficient is rather low in comparison with direct-gap semiconductors (such as GaAs and InP), which means that the absorption layer (base layer) of the solar cell must be made rather thick (0.2 mm to 0.5 mm) for a significant amount of the incoming light to be absorbed. The thickness of the silicon cells can be decreased, however, by using advanced light-trapping methods.

The highest recorded silicon cell conversion efficiencies have been reported for crystalline material. Crystalline silicon cells have been used since the first applications of power generation for satellites. The advantage of multicrystalline silicon material over crystalline is its lower price. The conversion efficiencies of cells made from it are lower, however, due to increased bulk recombination in this material.

Intensive silicon material research carried out in the 1930s and 1940s led to the development of the first practical solar cell of single crystal silicon at Bell Telephone Laboratories in 1954. These early cells were of $p$-on-$n$ junction type and had low energy conversion efficiency of 6%. The oil crisis in the beginning of the 1970s and the realization that fossil fuel sources were limited generated renewed interest in solar cell technology and since then it has made tremendous progress. Complex cell designs have been developed to increase the cell efficiency. Use of concentrated light approach on solar cells has been investigated. All these efforts were made to reduce the solar cell cost per watt of the produced power. The present single crystal silicon cell cost is more than 100 times lower than in late 1950s. At these levels many terrestrial applica-

tions became cost effective. To reduce the cost of solar cells, lower quality silicon, multicrystalline (partial ordering of atoms) and amorphous (random ordering of atoms) silicon materials were also developed. To further reduce the cost, screen printing process technology for fabricating solar cells was also commercialized.

However, to achieve highest cell efficiency one needs to use high purity silicon. Laboratory single crystal cells on relatively small area have resulted in efficiency of 24% under normal sunlight. There is a big difference in energy conversion efficiency between laboratory cell and large area silicon cells produced commercially. Normally the production cell efficiencies lie between 14% and 15%.

Multicrystalline silicon is a low purity material compared to single crystal silicon as multicrystalline silicon is grown by casting technique as compared to crystal pulling. Extensive development efforts made on this technology led to laboratory cell efficiencies approaching 18% under normal sunlight. These cells are very promising for many low-cost photovoltaic applications and are in commercial production.

### Advanced Crystalline Si Solar Cells

Silicon material and solar cells made from this material have made tremendous advances during the past 50 years. Work continues to further improve the performance of these cells by better design and processing. It is expected that silicon cells approaching 20% efficiency will be produced commercially for space use. The development of state-of-the-art microelectronic devices based on silicon technology and the strong awareness and demand for nonconventional energy sources have greatly improved silicon solar cell technology.

**Passivated-Emitter, Rear Locally Diffused Silicon Solar Cells.** The main loss mechanisms in conventional silicon solar cells are bulk and surface recombination, as well as interface recombination at the metal–semiconductor contacts. These recombination losses have been minimized in the PERL silicon solar cell, which holds the record for silicon cell conversion efficiency of 24% in the terrestrial AM1.5G spectrum (17) (see Table 2). In PERL cells, the bulk recombination is decreased, first of all, by achieving good bulk silicon crystal quality. If the trap level density is low, the dominating bulk recombination mechanism is Auger recombination. The radiative recombination processes are weak in silicon. The effect of surface recombination is reduced by good passivation of the cell emitter (cell front surface) by a thermally grown silicon dioxide layer. In metal–semiconductor contacts, the interface area is minimized (with point contacts) and the contact areas are heavily diffused to cause opposing electric fields in the contact regions to prevent minority carriers entering the contact area. Also, the low absorption coefficient of silicon leads to light penetration through the cell without absorption. In the PERL cell, this effect is decreased by enhancing the light trapping of the cell by using inverted pyramid surface texturing with asymmetric geometry, and back surface design for high reflection. In addition, the bulk SRH and Auger recombination losses of the cell are decreased by reducing the physical thickness of the cell; if the light can be absorbed in a thin structure, the minority carriers are collected before recombination even in material with poor diffusion length. Although these kind of cells have very good performance, approaching the theoretical limits of single-junction photovoltaic conversion with Si, the need for several lithographic steps in the process has hindered the commercial utilization of this design. The structure of the PERL cell is shown in Fig. 11.

In the gridless back-point-contact approach, both $n$- and $p$-type contacts are made on the back side of the Si cell, while the front surface is fully active and is textured (18). In this approach, the grid losses are totally avoided, and therefore such a cell is excellent from the point of view of concentrator applications.

### Thin Crystalline and Polycrystalline Si Cells

For terrestrial applications, the main driver has been to reduce the solar cell cost. During the last 25 years silicon solar cells became cost-effective for many applications due to advances in material and cell technology, and efforts are continuing. The cost of the starting silicon substrate is more than half of the solar cell cost. Due to their low absorption coefficient, crystalline silicon cells have to be made thick. To decrease the bulk crystal costs, one should reduce the thickness of the silicon substrate and enhance the absorption in this

**Table 2. Best Confirmed Solar Cell Conversion Efficiencies under AM1.5G Spectrum**

| Material | Eff. (%) | Area ($cm^2$) | Description (test year) |
|---|---|---|---|
| Si (crystalline) | 24.0 | 4.00 (ap) | PERL, UNSW (1994) |
| Si (thin crystalline) | 21.5 | 4.044 (ap) | 47 $\mu$m, UNSW (1995) |
| Si (multicrystalline) | 18.6 | 1.0 (ap) | Georgia Inst. of Tech. (1995) |
| Si (polycryst. thin film) | 9.4 | 1.0 (ap) | 3.5 $\mu$m on glass, Kaneka (1997) |
| Si (amorphous) | 12.7 | 1.0 (da) | Unstabilized, Sanyo (1992) |
| GaAs (crystalline) | 25.1 | 3.91 (t) | AlGaAs window, Kopin (1990) |
| InP (crystalline) | 21.9 | 4.02 (t) | Epitaxial, Spire (1990) |
| CdTe (polycrystalline) | 16.0 | 1.0 (ap) | 3.5 $\mu$m, Matsushita (1997) |
| $CuInGaSe_2$ (polycrystalline) | 17.7 | 0.41 (t) | On glass, NREL (1996) (Ref. 41) |
| GaInP/GaAs (crystalline) | 30.3 | 4.00 (t) | Double-junction, Japan Energy (1996) |
| a-SiC/a-Si/a-SiGe (amorph.) | 13.5 | 0.27 (da) | Triple-junction, unstab., USSC (1996) |

Results are collected from Ref. 40 unless otherwise noted.
Note: ap = aperture area, da = designated illumination area, t = total area, UNSW = University of New South Wales, NREL = National Renewable Energy Laboratory, USSC = United Solar Systems Corporation.

material. A solution to the problem is to use advanced light-trapping methods to confine the light inside a thin crystalline silicon cell. These cells may have thicknesses of the order of 50 $\mu$m, which is about one-fifth or less of the usual thickness. An efficiency of 21.5% has been demonstrated for a cell of this kind, which was only 47 $\mu$m thick (19). However, the manufacture of this cell needs several lithographic steps, thus limiting the commercialization of the device.

Thin silicon substrates in the form of ribbon or web have also been developed, but have not gained wide acceptance, due to various limitations. The approach of growing thin polycrystalline silicon films ($<$50 $\mu$m) on low-cost substrates has a high potential of reducing the amount of silicon used and providing a low-cost mechanical support for the solar cell. Light trapping is also used in thin film silicon cells to increase the absorption of light. Thin film silicon cells look quite promising for widespread terrestrial photovoltaic applications. A large number of research and development groups around the world are working on this approach.

Various methods have been used to deposit thin silicon films on different types of low-cost substrates, yielding efficiencies between 13% and 18%. Commercial production of high-efficiency thin silicon film cells will be a major breakthrough. This will greatly help in expanding the role of photovoltaic energy in meeting the ever increasing energy demand and improving the standard of living around the world in a cost-effective way. Other novel methods, such as spherical silicon cells, have been demonstrated but have not attracted much interest.

### Thin-Film Solar Cells

With thin-film solar cell materials one usually means a group of amorphous and polycrystalline semiconductors which have relatively high absorption coefficients and which can therefore be made of very thin layers for solar cell applications (20). Another common factor with these materials is the potential of very low cost of manufacturing. Due to the generally poor crystalline structure of these materials, the conversion efficiencies have remained relatively low, especially when constructed to large area modules. Significant global efforts are in progress to make these materials commercially viable. The best known material of this group is the hydrogenated amorphous silicon (a-Si : H), which has a significant portion of the world solar cell market, although it is mostly used in consumer applications such as watches and calculators. Other important materials of this group are chalcopyrites based on cadmium telluride (CdTe) and copper indium gallium sulfur selenide [Cu(In,Ga)(S,Se)$_2$, or CIGS].

Thin-film solar cells (except a-Si : H) are typically based on heterojunction $p$–$n$ structures (see Fig. 14). The absorber (base) layer is usually made a few micrometers thick, and it is covered with a thinner wide-gap window layer. The metallurgical $p$–$n$ heterojunction is formed in the interface between these layers, and the junction quality is typically not ideal due to a large amount of interface defects. To control the amount of the defects, a thin buffer layer may be used between the window and absorber layers. In addition, to decrease the effect of the defects as recombination centers, the electrical junction may be shifted away from the metallurgical junction by using highly $n$-doped window and low $p$-doped absorber layers.

**Hydrogenated Amorphous Silicon.** Hydrogenated amorphous silicon material (a-Si : H) has been believed to lead to lower solar cell manufacturing costs, since one needs a thin material layer compared to crystalline or multicrystalline silicon. This material is highly disordered and has large number of defects; therefore, efficiencies are quite low (4% to 5%). At these low efficiencies, it is not cost effective for various terrestrial applications. However, amorphous cells are very popular for consumer products (watches, calculators, battery charging, etc.). Amorphous cells work better under low intensity (indoor light) compared to single or polycrystalline silicon. Also it is possible to grow amorphous silicon on low-cost substrates (glass, plastic, metal) to reduce the thickness and weight of the cell. A problem with a-Si : H material is the Staebler–Wronski effect, which causes degradation of the material optoelectronic properties, decreasing the fill factor of the cell after illumination. The efficiency finally stabilizes, even in the best cases, to levels typically less than 10%.

Development work is under progress to improve the single junction amorphous silicon cell efficiency by adding more junctions. An experimental three junction small-area amorphous silicon cell having an efficiency of 13.5% (11% after stabilization) has been developed (13). The three material layers in this cell are formed of amorphous materials a-SiC : H, a-Si : H, and a-SiGe : H and connected by tunnel junctions. It is interesting to note that some other single junction thin-film materials have achieved efficiencies approaching 17%. This development suggests that it will be difficult for amorphous silicon cells to compete on an efficiency basis with other thin-film materials.

**Cadmium Telluride.** Cadmium telluride has a nearly optimum band-gap (1.4 eV) for terrestrial photovoltaic solar energy conversion. Due to the simple binary composition, it is easy to manufacture. Solar cells based on this material have a heterojunction structure, and the window layer is typically made of cadmium sulfide (CdS). The highest confirmed conversion efficiencies of these cells are in the range of 16%, but the reported submodule efficiencies are significantly lower (only 10% to 11%). A review of the CdTe solar cell technology can be found in Refs. 20–22.

**Copper Indium Diselenide and Related Alloys.** The material group of Cu(In,Ga)(S,Se)$_2$ (CIGS) chalcopyrite compounds have a wide range of band-gaps varying from 1.0 eV to 2.4 eV. $CuInSe_2$ (CIS) is the first material of this material group to have been used to make solar cells, although it has a non-ideal band-gap of only 1.0 eV. The band-gap of CIS can be increased by replacing part of the indium atoms with gallium atoms, and with this modification the conversion efficiencies have also increased. Some manufacturers replace also part of the selenium atoms with sulfur atoms. Due to these two degrees of freedom in the choice of the material composition, one may choose an ideal band-gap for the material while preserving a good lattice matching condition to the other materials used in the structure, which decreases the interface defect densities. Typically, these materials are grown on a glass substrate, and there are several methods which have been used for fabrication. References 20 and 23 have overviews of the status of CIGS technology.

### Solar Cell Materials Used in Space

Solar cells offer great potential for space (outside the Earth's atmosphere) applications, as sunlight is available most of the time except for brief eclipses. Moreover, solar cells are in many ways attractive compared with other sources of power such as electrochemical batteries or nuclear energy. Most of the communication and weather satellites in orbit are powered by solar cell arrays, without which we could not obtain up-to-date weather information or receive long-distance television broadcasts or telephone calls.

In space applications, some of the most important quality criteria for solar cells are different from those for cells that are used in terrestrial applications. Depending on the satellite's orbit, the space environment may be quite harsh, with extreme temperatures and ionizing radiation. Therefore, space solar cells are especially designed to withstand the space environment.

Maximum possible power per unit weight at the end of the life (EOL) of the satellite is the most important aim in the space solar cell development. The lowest possible weight of the panels is important, due to high weight-related launch costs. It costs approximately US $10,000 and US $45,000 to launch 1 kg of weight into low earth orbit (around 600 km above the earth) and geosynchronous orbit (36,000 km above the earth), respectively. Because it is usually impossible to replace the solar panels of the satellites after the launch to the orbit, one must consider the ionizing-radiation-induced degradation and the EOL power of the solar cells in space. Depending on the orbit of the satellite, the cells may experience heavy bombardment of high-energy electrons and protons, which originate from the sun and are trapped in the Van Allen belts in the earth's magnetosphere. If the satellite crosses the Van Allen belts, significant degradation of the cell conversion efficiency is expected. Therefore, the most important design criteria for space solar cells are high conversion efficiency and good radiation resistance, which should yield high power-to-weight ratio (as well as high power-to-area ratio) in the solar array.

The first solar cells for space applications were made of crystalline silicon in the late 1950s, thus marking the beginning of the modern photovoltaics era. Crystalline silicon was practically the only material used in space until the late 1980s, when solar cells based on the compound semiconductor gallium arsenide (GaAs) were introduced. GaAs has the advantage of a higher conversion efficiency than silicon, and it also has better radiation resistance. Typically, GaAs solar cells are grown on germanium (Ge) substrates. Germanium is somewhat cheaper than GaAs as a substrate material. It also has the advantage of being mechanically stronger than GaAs, which makes it possible to make the substrates thinner and therefore more lightweight. Due to its superior radiation resistance, another compound semiconductor, indium phosphide (InP), has had some interest for use in space applications. However, it has been used in only a few satellites because of its high cost.

The next generation space solar cells are the multijunction or cascade solar cells, which offer higher conversion efficiencies than single-junction silicon or GaAs cells. Double-junction GaInP–GaAs solar cells and triple-junction GaInP–GaAs–Ge cells belong to this newest group of space cells.

There has been also some interest in using thin film CIGS cells in space applications. Although these cells have relatively low conversion efficiencies, they have good radiation resistance, and they can be used to make very low-weight solar arrays having high power-to-weight ratios.

### Radiation Behavior of Semiconductor Materials and Solar Cells

The Van Allen belts touch the Earth's atmosphere in the polar regions, where the northern and southern lights are formed due to electron and proton collisions with the atmospheric molecules. Near the equator plane the belts are further away from the Earth. There are two main belts; the lower is located 1 to 3 Earth's radii from the Earth's surface (measured in the equator plane), and consists mainly of protons. The upper belt, formed mainly of electrons, extends about 5 to 10 Earth's radii from the surface. Energies of the typical electrons and protons trapped in the Van Allen belts are in the range of 1 MeV to 10 MeV.

Due to the existence of the Van Allen belts, there is an important additional quality requirement for solar cells if they are to be used as power sources for satellites. If the satellite's orbit crosses the Van Allen belts, the space solar cells must be radiation resistant, which means that their characteristics must deteriorate as little as possible when irradiated with high-energy electrons or protons. Depending on the satellite's orbit, however, the damage for the solar cells may vary a lot. Therefore, it is important to know what kind of damage for the solar cells is expected in every specific application.

Energetic protons and electrons cause vacancies, interstitials, and other defects throughout the active volume of the solar cell. If the volume of the cell is small, the number of defects in the cell is therefore also small. This is the main reason why compound semiconductor based solar cells have better radiation resistances than silicon. Due to the significantly lower absorption coefficient of Si, space solar cells based on this material are usually 10 to 50 times thicker than compound semiconductor based cells such as GaAs solar cells (excluding the substrate). However, there exist also other reasons for the differences in the radiation resistance between the compound semiconductors. Generally, phosphorus-containing semiconductor materials, such as InP, have better resistance than arsenic compounds, such as GaAs (24), and the resistance can vary significantly with doping level.

### End-of-Life Optimization of Space Cells

The solar panels must be designed in such a way that they will give enough power even at the EOL condition of the satellite, which may typically be up to 10 years from the launch. If there is a significant decrease of the panel power expected due to particle radiation during the satellite's lifetime, the panel must be oversized at the beginning-of-life (BOL) condition. This kind of situation increases the panel and launch costs. Therefore, the ideal design of the cell would mean high BOL conversion efficienices, and low degradation coefficients (EOL efficiency not very different from BOL efficiency).

With silicon cells, the difference between the BOL and EOL efficiencies can be made smaller by decreasing the cell thickness (i.e., decreasing the volume of the cells). This decreases the BOL efficiency, but may be advantageous on the system level due to diminished need for oversizing the panel.

GaAs solar cells have higher BOL efficiencies, and the relative degradation is about the same in comparison with thin Si space cells. Therefore, the EOL efficiencies are higher for GaAs cells than for Si cells, although Si technology is approaching that of GaAs in performance. The GaAs cell is less sensitive to temperature variation, which gives this technology a significant advantage in space application. In the case of multijunction GaInP/GaAs/Ge cells, the BOL efficiencies are still higher (typically well over 20% at AM0), and the relative degradation of the multijunction cells is limited by the GaAs subcell (for BOL optimized structure), giving the same relative degradation as single-junction GaAs cells. Therefore, the EOL efficiencies are still higher with these cells. The EOL optimization of the multijunction cells is more complicated than the single junction cells, because the current matching condition changes during the flight due to different degradation of the subcells. Because the GaAs cell degrades faster than the GaInP subcell, the BOL condition should be designed GaInP current limited, and the EOL condition should be current matched. With this kind of design, the relative degradation of the multijunction cell is defined by the good radiation resistance of the GaInP subcell, and the difference between the BOL and EOL conditions is minimized.

## Specific Space Solar Cell Materials

**Silicon Solar Cells for Space.** The first solar cell array was launched on March 17, 1958 aboard Vanguard I satellite. This solar cell array consisted of six small solar arrays or panels which were mounted on the body of the spacecraft. Each panel had 18 $p$-on-$n$ silicon solar cells of $2 \times 0.5$ cm$^2$ size and about 10% efficiency at 28°C. This solar cell array provided approximately 1 W of power for more than 6 years.

To date a few thousand satellites have been launched in space and the majority of these spacecrafts have used solar cell arrays as the primary source. From 1958 until the beginning of 1990s, single crystal silicon solar cells were the only cells used for space applications and will continue to be used in the future spacecrafts. In the past 40 years silicon solar cell size and efficiency have also improved significantly. Silicon cells of 17% energy conversion efficiency for space applications are in commercial production.

The assembly of the international space station will be completed by the year 2002. A 92 kW silicon solar cell array will provide the electric power to the station, 384 km above the Earth. The solar cells are $n$-on-$p$ type single crystal silicon of 8 cm $\times$ 8 cm size and 200 $\mu$m thick. The cells are approximately 15% efficient and each cell produces slightly more than 1 W of power. Therefore, thousands of solar cells connected in series and parallel will be used to meet the station's power requirement. This solar array is the largest one ever used in space.

**GaAs Solar Cells.** Gallium arsenide based solar cells have gained a significant proportion of the market in the satellite applications. In comparison to the previously dominating silicon solar cells, GaAs cells have significantly better BOL efficiencies and better radiation behavior. Using lattice-matched growth on Ge substrates, heteroepitaxial GaAs/Ge solar cells can be grown with quality approaching GaAs cells on GaAs substrates. Due to the lower cost and mechanical strength of Ge substrates, these heteroepitaxial GaAs/Ge cells are used exclusively. GaAs/Ge solar cells used in satellites have efficiencies of about 18% to 19% at AM0 conditions, and the best reported laboratory efficiencies are over 20% at AM0 for GaAs cells on both Ge and GaAs substrates.

GaAs material has a high surface recombination velocity. Using window layers with this material is therefore necessary. Wide-gap $Al_xGa_{1-x}As$ material is a natural choice for the window layer; it forms a well-behaving heterojunction with GaAs, and it is almost lattice-matched to GaAs with all values of $x$. The most important problem with the $Al_xGa_{1-x}As$ material is the high oxidation rate with high Al concentrations. Therefore, the highest possible value for $x$ is about 0.85.

**InP Solar Cells.** InP has a band-gap energy of 1.35 eV, close to the ideal band-gap energy, which makes it a material of choice for high-efficiency solar cells. It has been shown that InP solar cell efficiencies in excess of 24% at AM0 could be achieved if the surface recombination velocity could be reduced by a proper window layer (25). Solar cells based on InP material have very good radiation resistance, observed both for electron and proton irradiations (26). The good radiation behavior of InP can be explained by the self-annealing effect of phosphorus-containing semiconductor materials. In the past, InP solar cells have been flown on many flight experiments, and the results demonstrate their radiation superiority.

There exist, however, important drawbacks of InP as a solar cell material. There are no good choices for window layers (27); therefore the AM0 efficiency has remained below 20%. Other drawbacks of this material are its mechanical brittleness and high density, which cause problems in the reliability and launch costs in satellite applications. The high cost of this material is also a problem. Efforts are in progress to develop InP solar cells on low-cost mechanically strong substrates such as Si to reduce the cost and weight.

## Advanced Single Junction and Multijunction Solar Cells for Space Applications

Due to their larger bandgap energy, III–V semiconductor materials (GaAs, InP, etc.) offer higher energy conversion efficiencies than silicon solar cells at AM0. The III–V material substrates and their growth are many times more expensive than silicon or germanium substrates or related process technologies. Therefore, efforts are in progress to grow III–V materials either on silicon or germanium to reduce the starting III–V substrate cost.

Germanium is more expensive than silicon, but is lattice-matched to GaAs. GaInP–GaAs dual-junction and GaAs single-junction solar cells grown on Ge substrates are in commercial production. GaInP–GaAs–Ge three-junction solar cells grown on Ge substrate have been produced in the laboratory (28). However, GaAs is lattice-mismatched to silicon, and InP is lattice-mismatched to both silicon and germanium. Therefore, the growth of III–V materials under mismatch conditions will be accompanied by a large generation of defects or misfit dislocations. These dislocations are catastrophic to the performance of the solar cell (29). Several approaches are under investigation to reduce the number of defects.

To achieve well over 20% conversion efficiencies for space applications, multijunction solar cells have been developed.

Materials for multijunction cells are based on GaInP–GaAs–Ge and InP–GaInAs systems. The GaInP–GaAs–Ge cells are grown on Ge substrates, and the Ge may be either passive or active. In structures having passive Ge, the polarity is usually *p*-on-*n*, and the cell consists of a two-junction GaInP–GaAs structure. In triple-junction cells having active Ge junctions, the solar spectrum can be used more efficiently (see Fig. 15), and a few percent increase is expected in the conversion efficiencies in comparison with the double-junction structures. The Ge junction is formed during growth of GaAs. Interdiffusion of Ge and GaAs can occur during the growth of all subsequent layers.

The double-junction GaInP–GaAs cells on GaAs substrates have yielded nearly 27% AM0 efficiencies (30), and they are the first reported monolithic two-terminal solar cells that have yielded over 30% conversion efficiencies under a 1-sun AM1.5G spectrum.

Although the InP–GaInAs double-junction structures have yielded significantly higher efficiencies (31) than epitaxially grown and diffused (32) single-junction InP solar cells, no cost-effective, mechanically strong Ge-like substrate exists. These structures are grown on InP substrates, and therefore the same mechanical and cost-related problems arise as with single-junction InP cells.

## CONCENTRATOR SOLAR CELLS

Using concentrated sunlight provides several advantages in photovoltaic conversion, of which the most important are the increased conversion efficiencies of the solar cells, and savings in panel costs due to the smaller needed solar cell area. The cell current and consequently power generated will increase proportionally with the intensity of the sunlight. In the concentrator approach, lenses or mirrors are used to concentrate sunlight on solar cells. There exist several concentrator types, of which the point focus and linear focus are the most common ones using refractive optics. Parabolic dish mirrors are examples of concentrators applying reflective optics. For space applications, the concentrator modules may be inflatable to minimize the needed volume during launch.

In concentrator systems, the expensive solar cells are partly replaced by the optical elements, with resulting reduction. The cost reduction depends on the complexity of the concentrator system. Despite various claims, this approach has not yet been widely used, but it is gaining more acceptance for both terrestrial and space applications. Several demonstration projects based on this approach are in operation. In concentrator applications, solar cells of the highest possible efficiencies are required to take advantage of the high-intensity sunlight.

The main drawbacks of the concentrator systems are that for maximum performance, some kind of tracking of the sun's daily motion is needed, as well as cooling of the cells. The higher the concentration is, the more accurate the tracking must be. Although the tracking provides several advantages, the consequences of the need for tracking are increased maintenance costs, and almost zero output in cloudy weather.

For very low concentration, the system can be made nontracking by using reflector plates around the solar panels. Passively tracking systems normally have one axis of rotation, and their performance is therefore better than that of nontracking systems, but still only low concentration levels can be used. Active tracking usually means that the system has two axes of rotation, and the panels are directed accurately toward the sun by using microprocessor control. The advantages of active tracking are the high possible concentration (up to several hundred suns) and the high effective usage of the available solar light because the panels are always optimally directed towards the sun.

If the intensity of the solar radiation is increased by the means of optical concentration, higher conversion efficiencies for solar cells are expected. That is because the output voltage, which is related to the photocurrent density, increases with the light intensity [i.e., the photocurrent; see Eq. (5)] and also the fill factor increases, because the relative effect of the forward diffusion current decreases with increasing photocurrent [Eq. (2)]. With increasing output currents, however, the resistive losses in the solar cell also increase. Therefore, the series resistance of the concentrator cells has to be decreased in comparison with typical solar cells using nonconcentrated solar light. The grid design, ohmic contacts between the metal and semiconductor, emitter sheet resistance, and base series resistance have to be redesigned.

A record high efficiency of 27.5% was demonstrated for silicon solar cells at 100-sun concentration. This cell had both contacts on the back side and has been referred to as a backside point-contact solar cell (18). More expensive crystalline compound semiconductor solar cells, such as GaAs single-junction cells, can be used in concentrator applications. GaAs–GaSb, InP–GaInAs, and GaInP–GaAs multijunction cells have shown over 30% efficiencies under terrestrial concentrator (see Table 3), a result that makes these cells interesting for terrestrial applications in addition to space use. Cell- and optics-related work is progressing to further improve the efficiencies for concentrator applications. Reference 33 overviews the concentrator cell physics and technology.

**Table 3. Best Confirmed Concentrator Cell Conversion Efficiencies under AM1.5D Spectrum**

| Material | Efficiency (%) | Concentration (suns) | Area ($cm^2$) | Description (year) |
|---|---|---|---|---|
| GaAs | 27.6 | 255 | 0.126 (da) | Spire (1991) |
| InP | 24.3 | 99 | 0.075 (da) | NREL (1991) |
| Si | 28.2 | 100 | 0.15 (da) | Stanford University (1987) (Ref. 42) |
| GaAs/GaSb | 32.6 | 100 | 0.053 (da) | Mechanical stack, Boeing (1989) |
| InP/GaInAs | 31.8 | 50 | 0.063 (da) | Monolithic, triple-terminal, NREL (1990) |
| GaInP/GaAs | 30.2 | 180 | 0.103 (da) | Monolithic, double-terminal, NREL (1994) |

Results collected from Ref. 35 unless otherwise noted.
Note: da = designated illumination area, NREL = National Renewable Energy Laboratory.

## NONSOLAR APPLICATIONS FOR PHOTOVOLTAIC CELLS

This section briefly discusses the devices that generate electricity from thermal and laser sources instead of sunlight. Hence we refer to these devices as photovoltaic cells and not solar cells, although these cells amount to specially designed solar cells. The detailed description of these new types of cells is beyond the scope of this article.

### Thermophotovoltaic Cells

A relatively new nonsolar photovoltaic application is thermophotovoltaic (TPV) conversion. In this case the incoming radiation is in the infrared part of the spectrum.

Cells for this purpose directly convert thermal energy into electrical energy. This effect was discovered more than 30 years ago, but the recent developments in material growth technology have generated renewed interest in this field. TPV power generators offer many advantages and could be used for a wide range of applications, similar to solar PV generators. TPV systems can be operated by combustion, radioisotopes, and even solar energy. In a typical TPV system, the source heat is transmitted to the TPV cell through selective emitter material, which filters and converts the source radiation wavelength range to better match with the response of the TPV cell. Modeling studies (34) have predicted TPV cell efficiencies in excess of 30%, depending on the source temperature. High-temperature sources offer a large power density, but source heat management and uniformity, temperature limitations of materials, keeping the cells clean, and cooling of the cells pose problems. Sources between 1000 K and 2000 K offer a good possibility for terrestrial as well as space TPV applications. Cells of narrow-band-gap materials in the range of 0.5 eV to 0.74 eV are suitably matched to the spectrum of the sources between 1000 K and 2000 K. Cells of indium gallium arsenide, gallium antimonide, and related materials are being developed for TPV applications. These materials have relatively high cost; therefore silicon has also been considered as a candidate material for TPV application, although this material has a nonideal wavelength response range.

### Monochromatic Photovoltaic Power Conversion

Solar cells can exhibit higher efficiency under monochromatic light than under solar illumination. If the incoming radiation onto the photovoltaic cell consists only of a narrow spectrum just above the band edge of the cell, the phonon emission and photon transmission losses are minimized. Theoretically, conversion efficiency of over 60% is expected for a GaAs-based monochromatic photovoltaic converter if the photon energy is only slightly larger than the material band-gap, and experimental devices have yielded over 50% efficiencies (35).

Light-to-electric power converters are used in applications where good galvanic insulation is needed. Such an application is, for example, a sensor located in an environment having explosive gases or high voltages. By using a monochromatic photovoltaic converter, the electrical power for the sensor electronics is transferred in the form of laser emission light and can therefore be guided via an optical fiber.

## MANUFACTURING OF SOLAR CELLS

The solar cell manufacturing process can be divided in two basic parts. In the first step, the solar cell material is grown. Usually formation of the $p$–$n$ junction is included in the material growth process. An exception is the Si cell process, where the $p$–$n$ junction is formed subsequently by diffusion after the material growth process. The second step in the manufacturing process is the contact formation, consisting of the front contact grid and back contact deposition, and the AR-coating formation. A comprehensive overview of the manufacturing technologies of solar cells is given in Ref. 11.

### Material Growth

In the case of crystalline silicon, the bulk crystal is usually grown by using the Czochralski growth method. In this method, the silicon crystal is pulled from a silicon melt and crystallized by using a seed crystal in such a way that the orientation of the seed crystal is copied to the bulk crystal. The bulk crystal is then sliced to wafers, having a thickness of the order of 0.5 mm. These wafers are then etched to remove the crystal damage from the wafer surface caused by the slicing process. The quality of the single crystal silicon wafers grown by the Czochralski method is good, but the material cost is too high for large-scale solar power applications, except in concentrator configurations. In practice, the cost of the Si material can be kept low by using low-grade Si products from the electronics industry. Multicrystalline silicon is used in many cases because the manufacturing process cost of this material is significantly lower compared to single crystal silicon. To produce multicrystalline silicon, small pieces of crystalline silicon are put together in a mold and melted. When the melt is slowly solidified, a multicrystalline ingot (grain size more than 1 mm) is formed.

Thin-film materials are typically deposited from gaseous sources, which react to form the desired compounds on a specific substrate. The most important two chemical deposition techniques are spray pyrolysis and chemical vapor deposition (CVD) processes. With these methods, silicon material grows in polycrystalline (grain size less than 1 mm) or amorphous form. Chalcopyrite materials and other thin-film compound semiconductors are grown in polycrystalline form.

High-efficiency crystalline compound semiconductor materials, such as GaAs and GaInP, are grown by epitaxial growth methods. In solar cell applications, large-throughput epitaxial growth systems are needed. Of these, the metalloorganic vapor phase epitaxy (MOVPE, also known as metalloorganic chemical vapor deposition, or MOCVD) is the most typically used method. However, other epitaxial growth methods such as liquid-phase epitaxy (LPE) and molecular beam epitaxy (MBE) have also been used or considered for solar cell production.

### Patterining and Contact Formation

The grid patterining for the solar cells can be made by using conventional optical lithography methods. Optical lithography enables manufacturing of narrow finger patterns, but is relatively slow method due to the many steps needed in the process, such as resist deposition, hardening of the resist, mask alignment and exposure, resist development, metal evaporation and lift-off. Due to the complexity of this process, it is only used for expensive concentrator cells and space cells. For inexpensive large-scale production, a simpler screen printing process has been developed. In the screen printing method,

the metal grid pattern is pasted on the solar cell surface with a relatively simple mechanical printing machine.

The back metal contact usually does not need any kind of patterning. The metal layers may be deposited by evaporation or sputtering methods, or by electrochemical plating. Both front and back metal contacts may need thermal annealing to achieve ohmic contacts between the metal and the semiconductor layers.

### Health Issues Related to Solar Cell Manufacturing

There is some concern about the toxicity of some of the materials which are used in the manufacturing of thin-film cells. As is in the case of basically all semiconductor manufacturing processes, toxic gases and chemicals have to be used in the fabrication of thin-film solar cells. The risks for the manufacturing personnel can be minimized, however, with proper safety practices. In the case of CdTe solar panels, also the panel disposal and recycling have to be arranged at the end of the lifetime of the panels (which may typically be 20 to 30 years), due to the toxicity of cadmium and tellurium. There is normally no health hazard risks in the use of the panels. An assessment of the health risks in solar cell technology is made in Ref. 36.

## CHARACTERIZATION OF SOLAR CELLS

Usually, the most important parameter for the user of the solar cell is the output power. Determination of the conversion efficiency of the solar cell, which can be determined by load-IV measurements, defines the quality of the device in this respect. However, there are other characterization techniques which are important in the development process of the solar cell. Measurement of the spectral response and the quantum efficiency describe the photocurrent generation properties of the cell. Dark-*IV* characteristics determine the quality of the $p$–$n$ junction. Reflection measurement defines the properties of the AR coating. Minority carrier lifetime measurements, electroluminescence measurements, and electron beam induced current measurements give useful information about the semiconductor material quality. An overview of the characterization procedures of solar cells can be found in Ref. 37.

### Measurement of Load-IV Characteristics

To reliably determine the current-voltage characteristics of a solar cell, one needs accurate simulation of the standard solar spectrum at the given air mass conditions. However, all solar simulators give only approximate reproductions of the solar spectrum. The simulators are usually based on xenon lamps, which roughly represent the black body emission spectrum at 5800 K. These lamps give strong output at ultraviolet wavelengths and also characteristic peaks at longer wavelengths. The light output of the lamp is usually filtered to adjust for the desired air mass condition. It is especially important to have a correct simulator spectrum when multijunction cells are measured, because the current matching condition is of crucial importance in these structures. Therefore, the most accurate measurements for multijunction structures are obtained with multisource simulators, in which the subcells are separately light-biased with the aid of spectrally selective lamps.

In the load-*IV* curve measurement, the lamp intensity has to be set to the standard condition with the aid of a calibrated standard cell, and the cell temperature must be accurately controlled. To eliminate resistance errors originating from contacting the cell with measurement probes, the four-contact-probe method is preferred. The *IV*-curve can then be determined by varying the load resistor value. The reference cell calibration can be made in near-AM0 conditions at high-altitude balloon or aircraft flights, or even in spacecraft flights. These primary-calibrated cells can then be used to make secondary calibration standards, which can be used for normal solar cell testing.

### Dark-IV Characteristics

Measurement of the dark-*IV* characteristics of a solar cell gives valuable information about the $p$–$n$ junction quality. This measurement requires a current–voltage source and corresponding meters. Use of a four-point contacting scheme improves the accuracy of the measurement. Characterization of the dark current at the bias voltage near the power maximum point is most usable, but voltage regions where recombination and diffusion currents are dominating can also be determined. The existence of traps in the depletion region can be observed from the ideality factor determined from the *IV* curve. In addition, shunt and series resistance values can be measured, for example, to reveal the reasons for a low fill factor. From the difference in the dark and load *IV* characteristics one can also define the possible contribution of the interface recombination to the photocurrent losses. For thin-film solar cells especially, a lot of information is obtained by looking at the change in the $I$–$V$ curve shape with variable-intensity light bias.

### Quantum Efficiency Measurements

The quantum efficiency of a solar cell can be measured with a system having a white light source and a set of band-pass filters or a monochromator, a current amplifier, and a calibrated reference cell. The cell response is then scanned with various wavelengths and compared with the reference cell response. The quantum efficiency can thus be calculated. In the case of multijunction cells, the quantum efficiency measurements have to be performed separately for each subcell by light biasing the other cells in the structure in such the way that the subcell to be measured is the current limiting cell (38). For nonideal devices (especially thin-film cells) the QE may depend on the light intensity and on the bias voltage. Comparison of the QE measured at low light levels with that at 1-sun light levels, and of the QE at short-circuit conditions with that at forward voltage bias, can give clues about the loss mechanisms in the cell.

The direct result of the quantum efficiency measurement is the external QE. To define the internal QE, one has to measure also the reflectance of the solar cell as a function of the wavelength. The internal QE can then be calculated.

### Minority Carrier Lifetime Measurements

Rough estimations about the minority carrier lifetimes of the solar cell materials can be made from the quantum efficiency measurements. Comparing with numerical modelling of the quantum efficiency, for example with PC-1D program (39),

**Table 4. Best Reported Solar Cell Efficiencies under One-Sun Space AM0 Spectrum**

| Structure | Eff. (%) | Area ($cm^2$) | Description (year) (Ref.) |
|---|---|---|---|
| Si | 18.3 | 4 (t) | Sharp (1993) (43) |
| GaAs | 22.5 | 4 (t) | Mitsubishi (1987) (44) |
| GaAs/Ge (single-junction) | 20.5 | 4 (t) | ASEC (Tecstar) (1990) (45) |
| InP | 19.1 | 4 (t) | Spire (1990) (9) |
| InP/GaInAs (double-junction) | 22.2 | 1 (t) | NREL (1994) (31) |
| GaInP/GaAs (double-junction) | 26.9 | 4.00 (t) | Japan Energy (1998) (30) |
| GaInP/GaAs/Ge (double-junction) | 24.2 | 0.25 (t) | Spectrolab (1994) (46) |
| GaInP/GaAs/Ge (triple-junction) | 25.7 | 4 (t) | Spectrolab (1996) (28) |

Note: t = total area, ASEC = Applied Solar Energy Corporation, NREL = National Renewable Energy Laboratory.

one may obtain approximations for the carrier lifetimes. This method can be used if the other material parameters are known, such as the surface and interface recombination velocities and the absorption coefficient. However, typically there are not enough data about these parameters for many important new materials, therefore numerical modeling may not be a reliable method of minority carrier lifetime determination.

Minority carrier lifetimes in solar cell materials are usually defined by photoluminescence decay measurements. In this method, short laser pulses are aimed at the material, and the luminescence decay is measured as a function of time. Different recombination lifetimes can then be obtained from the decay curve slopes. The problem with this method is that the light intensity of the laser pulse is very high in comparison to the normal solar light intensity, and the recombination mechanisms depend strongly on the light intensity. Another drawback is the fact that many recombination mechanisms are nonradiative. Therefore, one can only make estimations about the relevant decay characteristics in the actual solar cell operation environment.

Electron-beam induced current (EBIC) is also relevant method for giving qualitative information about the minority carrier lifetimes. In this method, an electron beam is scanned over the solar cell, and the induced current as a function of position of the beam can be mapped. This method is sensitive to small variations in the minority carrier properties of the material, but does not give quantitative values for the lifetimes, and it cannot be used for minority hole property measurements.

## CURRENT STATUS OF SOLAR CELL EFFICIENCIES

The record conversion efficiencies of the most important terrestrial solar cells under 1-sun, AM1.5G conditions, are listed in Table 2, and concentrator cell results for AM1.5D spectrum are listed in Table 3. For space solar cells, the best reported conversion efficiencies are shown in Table 4. The source for the AM1.5 efficiencies is the efficiency tables published in Ref. 40, and the references for the AM0 results are shown in the reference column of the Table 4.

The record efficiencies listed in the tables are all laboratory results, and the real solar cell production efficiencies are in many cases significantly lower. However, the research and development of semiconductor materials and solar cells are continually yielding higher efficiencies both in the laboratory and in manufacturing, at the same time as the cell costs are decreasing. Therefore, one may expect growing markets for solar cells and increased utilization of solar energy with photovoltaics in the future.

## BIBLIOGRAPHY


1. L. L. Kazmerski, Status and assessment of photovoltaic technologies, *Int. Mater. Rev.,* **34**: 185–210, 1989.
2. J. J. Loferski, The first forty years: A brief history of the modern photovoltaic age, *Progress Photovolt.,* **1**: 67–78, 1993.
3. M. A. Green, *Silicon Solar Cells, Advanced Principles and Practice,* Sydney: Univ. New South Wales, 1995.
4. S. R. Wenham, M. A. Green, and M. E. Watt, *Applied Photovoltaics,* Centre for Photovoltaic Devices and Systems, Sydney: Univ. New South Wales, 1994.
5. H. J. Hovel, Solar cells, in *Semiconductors and Semimetals,* vol. 11, New York: Academic Press, 1975.
6. S. M. Sze, *Physics of Semiconductor Devices,* 2nd ed., New York: Wiley, 1981.
7. M. A. Green, *Solar Cells, Operating Principles, Technology and System Applications,* Englewood Cliffs, NJ: Prentice-Hall, 1982.
8. S. R. Kurtz, J. M. Olson, and A. Kibbler, High efficiency GaAs solar cells using $GaInP_2$ window layers, *Conf. Rec. 21st IEEE Photovolt. Specialists Conf.,* 1990, pp. 138–141.
9. C. J. Keavney, V. E. Haven, and S. M. Vernon, Emitter structures in MOCVD InP solar cells, *Conf. Rec. 21st IEEE Photovolt. Specialists Conf.,* 1990, pp. 141–144.
10. D. L. Meier and D. K. Schroder, Contact resistance: Its measurement and relative importance to power loss in a solar cell, *IEEE Trans. Electron Devices,* **ED-31**: 647–653, 1984.
11. K. L. Chopra and S. R. Das, *Thin Film Solar Cells,* New York: Plenum, 1983.
12. S. S. Li, *Semiconductor Physical Electronics,* Plenum Press, 1993.
13. S. Guha et al., Amorphous silicion alloy photovoltaic technology—from R&D to production, *Mater. Res. Soc. Symp. Proc.,* **336**, 1994.
14. L. M. Fraas et al., Over 35-percent efficient GaAs/GaSb tandem solar cells, *IEEE Trans. Electron Devices,* **37**: 443–449, 1990.
15. T. Takamoto et al., Over 30% efficient InGaP/GaAs tandem solar cells, *Appl. Phys. Lett.,* **70**: 381–383, 1997.
16. K. A. Bertness et al., 29.5%-efficient GaInP/GaAs tandem solar cells, *Appl. Phys. Lett.,* **65**: 989–991, 1994.
17. J. Zhao et al., 24% efficient silicon solar cells with double layer anti-reflection coatings and reduced resistance loss, *Appl. Phys. Lett.,* **66**: 3636–3638, 1995.
18. R. A. Sinton et al., 27.5-percent silicion concentrator solar cells, *IEEE Electron Dev. Lett.,* **EDL-7**: 567–569, 1986.
19. A. Wang et al., 21.5% efficient thin silicon solar cell, *Progress Photovolt.,* **4**: 55–58, 1996.

20. W. H. Bloss et al., Thin film solar cells, *Progress Photovolt.,* **3**: 3–24, 1995.
21. P. V. Meyers and R. W. Birkmire, The future of CdTe photovoltaics, *Progress Photovolt.,* **3**: 393–402, 1995.
22. T. L. Chu, Cadmium telluride solar cells, in T. J. Coutts and J. D. Meakin (eds.), *Current Topics in Photovoltaics,* vol. 3, London: Academic Press, 1988.
23. V. Nadenau et al., Solar cells based on $CuInSe_2$ and related compounds: Material and device properties and processing, *Progress Photovolt.,* **3**: 363–382, 1995.
24. M. Yamaguchi et al., Radiation resistance of InGaP solar cells, *Conf. Rec. 25th IEEE Photovolt. Specialists Conf.,* 1996, pp. 163–166.
25. R. K. Jain and D. J. Flood, Effects of recombination parameters in $p + n$ indium phosphide solar cells, *Solar Energy Mater. and Solar Cells,* **45**: 51–55, 1997.
26. T. J. Coutts and M. Yamaguchi, Indium phosphide-based solar cells: A critical review of their fabrication, performance and operation, in T. J. Coutts and J. D. Meakin (eds.), *Current Topics in Photovoltaics,* vol. 3, London: Academic Press, 1988.
27. J. Lammasniemi, K. Tappura, and K. Smekalin, Recombination mechanisms at window/emitter interface in InP and other III-V semiconductor-based solar cells, *1st World Conf. Photovolt. Energy Conversion,* Institute of Electrical and Electronics Engineers, 1994, pp. 1771–1774.
28. P. K. Chiang et al., Experimental results of $GaInP_2$/GaAs/Ge triple junction cell development for space power systems, *Conf. Rec. 25th IEEE Photovolt. Specialists Conf.,* Institute of Electrical and Electronics Engineering, 1996, pp. 183–186.
29. R. K. Jain and D. J. Flood, Influence of the dislocation density on the performance of heteroepitaxial indium phosphide solar cells, *IEEE Trans. Electron Devices,* **40**: 1928–1929, 1993.
30. T. Takamoto et al., High-efficiency radiation-resistant InGaP/GaAs tandem solar cells, *Conf. Rec. 26th IEEE Photovolt. Specialists Conf.,* 1997.
31. M. W. Wanlass et al., Improved large-area, two-terminal $InP/Ga_{0.47}In_{0.53}As$ tandem solar cells, *1st World Conf. Photovolt. Energy Conversion,* Institute of Electrical and Electronics Engineers, Inc., 1994, pp. 1717–1720.
32. M. Yamaguchi et al., *Appl. Phys. Lett.,* **44**: 432–434, 1984.
33. V. M. Andreev, V A. Grilikhes, and V. D. Rumyantsev, *Photovolt. Conversion Concentrated Sunlight,* Chichester: Wiley, 1997.
34. R. K. Jain et al., Lattice matched and strained InGaAs solar cells for thermophotovoltaic use, in J. P. Benner, T. J. Coutts, and D. S. Ginley (eds.), *Proc. 2nd NREL Conf. Thermophotovoltaic Generation of Electricity,* American Institute of Physics, 1996, pp. 375–386.
35. L. C. Olsen et al., High efficiency monochromatic GaAs solar cells, *Conf. Rec. 22nd IEEE Photovolt. Specialists Conf.,* 1991, pp. 419–424.
36. P. D. Moskowitz, An overview of environmental, health, and safety issues in the photovoltaic industry, in L. D. Partain (ed.), *Solar Cells and Their Applications,* New York: Wiley, 1995.
37. K. A. Emery and C. R. Osterwald, Efficiency measurements and other performance rating methods, in T. J. Coutts and J. D. Meakin (eds.), *Current Topics in Photovoltaics,* vol. 3, London: Academic Press, 1988.
38. S. R. Kurtz, K. Emery, and J. M. Olson, Methods for analysis of two-junction, two-terminal photovoltaic devices, *1st World Conf. Photovolt. Energy Conversion,* Institute of Electrical and Electronics Engineers, 1994, pp. 1733–1737.
39. P. A. Basore and D. A. Clugston, PC1D Version 4 for Windows, from analysis to design, *Conf. Rec. 25th IEEE Photovolt. Specialists Conf.,* Institute of Electrical and Electronics Engineers, 1996, pp. 377–382.
40. M. A. Green et al., Solar cell efficiency tables (Version 10), *Progress Photovolt.,* **5**: 265–268, 1997.
41. K. Zweibel, H. S. Ullal, and B. von Roedern, Progress and issues in polycrystalline thin-film PV technologies, *Conf. Rec. 25th IEEE Photovolt. Specialists Conf.,* 1996, pp. 745–750.
42. R. A. Sinton, Terrestrial silicon concentrator solar cells, in L. D. Partain (ed.), *Solar Cells and Their Applications,* New York: Wiley, 1995.
43. H. Washio et al., Development of high efficiency thin silicon space solar cells, *Conf. Rec. 23rd IEEE Photovolt. Specialists Conf.,* 1993, pp. 1347–1351.
44. N. Ogasawara et al., 22.5-percent (one-sun, AM0) GaAs solar cell with AlGaAs/GaAs superlattice buffer layer, *Tech. Dig. 3rd Int. Photovolt. Sci. Eng. Conf.,* 1987, p. 477.
45. P. A. Iles et al., High-efficiency (>20% AM0) GaAs solar cells grown on inactive-Ge substrates, *IEEE Electron Dev. Lett.,* **11**: 140–142, 1990.
46. P. K. Chiang et al., Large area $GaInP_2$/GaAs/Ge multijunction solar cells for space applications, *1st World Conf. Photovolt. Energy Conversion,* Institute of Electrical and Electronics Engineers, 1994, pp. 2120–2123.

JOUKO LAMMASNIEMI
Tampere University of Technology
RAJ K. JAIN
Space Systems/Loral